

**INTERACTIONS OF CHOLINERGIC INNERVATION AND SOLUBLE AB42  
PEPTIDE METABOLISM IN THE HIPPOCAMPUS**

by

Barbara Anna Isanski

B.S., University of Pittsburgh, 2001

Submitted to the Graduate Faculty of  
The School of Medicine in partial fulfillment  
of the requirements for the degree of  
Master of Science

University of Pittsburgh

2007

UNIVERSITY OF PITTSBURGH

School of Medicine

This thesis was presented

by

Barbara Anna Isanski

It was defended on

December 14, 2007

and approved by

Patrick Card, PhD, Department of Neuroscience

Teresa Hastings, PhD, Department of Neurology

Thesis Advisor: Steven T. DeKosky, MD, Department of Neurology

# **Interactions of cholinergic innervation and soluble A $\beta$ 42 peptide metabolism in the hippocampus**

Barbara Anna Isanski

University of Pittsburgh, 2007

Alzheimer's Disease (AD) is a chronic neurodegenerative disorder characterized clinically by dementia and neuropathologically by the presence of amyloid- $\beta$  (A $\beta$ ) plaques, neurofibrillary tangles, and neuronal and synapse loss. AD dementia severity correlates with reductions in synapses as well as in cholinergic markers, including choline acetyltransferase (ChAT) and acetylcholine esterase (AChE). However, the exact relationship of these changes with A $\beta$  metabolism and plaques is unclear. Recently, it has been proposed that reduced cholinergic activity can increase levels of A $\beta$  peptide. We investigated this relationship using a well-characterized model of hippocampal cholinergic denervation (achieved by fimbria-fornix transection) in a unique human A $\beta$  "knock-in" mouse model of AD. The fimbria fornix lesion was effective in diminishing the cholinergic input to the hippocampus; ChAT immunoreactive fiber densities were reduced in the hippocampus, and cholinergic enzyme activity levels were reduced by almost 50% compared to naïve animals. Fimbria fornix lesions also resulted in a 3-fold increase in soluble A $\beta$ 42 over naïves, supporting the hypothesis that loss of cholinergic innervation increases A $\beta$  peptide levels in target fields. Our data indicate that cholinomimetic therapies could prove valuable in suppressing increases in potentially neurotoxic soluble A $\beta$  levels, and provide a model for evaluating *in vivo* the relationship between cholinergic function and amyloid metabolism.

## TABLE OF CONTENTS

<b>1.0</b>	<b>INTRODUCTION.....</b>	<b>1</b>
1.1.1	Amyloid precursor protein (APP) and the production of A $\beta$ : amyloidogenic and non-amyloidogenic pathways.....	2
1.1.2	Anatomy of the cholinergic system.....	3
1.1.3	Biochemistry of the cholinergic system.....	5
1.1.4	Animal models of cholinergic dysfunction.....	5
1.1.5	Cholinergic deficits in Alzheimer’s Disease.....	6
1.1.6	Relationship between cholinergic neurotransmission and APP processing.....	7
1.1.7	Cholinergic dysfunction in mouse models of AD.....	9
1.1.8	Fimbria fornix lesioned humanized A $\beta$ mouse: cholinergic-amyloid interactions.....	10
<b>2.0</b>	<b>METHODS.....</b>	<b>12</b>
2.1.1	Humanized A $\beta$ mice.....	12
2.1.2	Fimbria fornix lesion.....	12
2.1.3	Nissl Stain.....	13
2.1.4	Luxol Fast Blue.....	13
2.1.5	AChE Histochemistry.....	14

2.1.6	ChAT Immunocytochemistry .....	15
2.1.7	Analysis of ChAT-immunoreactive fiber density.....	15
2.1.8	AChE Activity Assay .....	16
2.1.9	ChAT Activity Assay .....	18
2.1.10	Soluble A $\beta$ 42 ELISA.....	19
2.1.11	BCA Protein Assay .....	21
2.1.12	Statistics .....	21
3.0	RESULTS .....	23
3.1.1	Histological verification of the fimbria fornix lesions .....	23
3.1.2	Fimbria fornix lesion results in reduced densities of cholinergic fibers in the hippocampus: AchE histochemistry and ChAT immunocytochemistry .....	25
3.1.3	Fimbria fornix lesion results in loss of hippocampal AChE activity.....	27
3.1.4	Fimbria fornix lesion results in loss of hippocampal ChAT activity.....	29
3.1.5	Fimbria fornix lesion results in increased soluble A $\beta$ 42 levels in hippocampus.....	31
3.1.6	Correlative analyses.....	32
4.0	DISCUSSION .....	35
	REFERENCES.....	40

## LIST OF TABLES

Table 1 Fimbria-fornix lesion results in decreased ChAT-ir fiber density in hippocampus .....	24
Table 2 Fimbria fornix lesion results in decreased cholinergic enzyme activity and increased soluble A $\beta$ 42 levels.....	27

## LIST OF FIGURES

Figure 1 Histological proof of proper lesion placement. ....	24
Figure 2. Histochemical and immunohistochemical evidence of fimbria fornix lesion efficacy. .	26
Figure 3 The effect of fimbria fornix lesion on ChAT-immunoreactive fiber density in the hippocampus. ....	28
Figure 4. The effect of fimbria fornix lesion on AChE activity in hippocampus. ....	29
Figure 5. The effect of fimbria fornix lesions on ChAT activity in hippocampus. ....	30
Figure 6. Effect of bilateral fimbria-fornix on soluble A $\beta$ 42 levels in hippocampus. ....	31
Figure 7. ChAT activity increases as AChE activity increases. ....	32
Figure 8. Soluble A $\beta$ 42 levels increase as AChE activity decreases. ....	33
Figure 9. Soluble A $\beta$ 42 levels increase as ChAT activity decreases. ....	34

## 1.0 INTRODUCTION

Alzheimer's Disease (AD) is a chronic neurodegenerative disorder characterized clinically by dementia and neuropathologically by the presence of amyloid plaques and neurofibrillary tangles (Selkoe DJ, 2005). Another common neuropathological finding in AD brains is neuronal loss, notably in the cholinergic basal forebrain (Whitehouse PJ et al, 1982), the region providing major cholinergic input to the hippocampus and neocortex (Mesulam MM et al, 1983). Neuronal loss in AD brains is associated with a loss of synapses (Scheff SW et al, 1990), which correlates directly with cognitive impairment (DeKosky ST and Scheff SW, 1990). However, the exact nature of the relationship between cholinergic synaptic deficits and the major neuropathological hallmarks of the disease (e.g., amyloid plaques) is unclear. Recently, it has been proposed that a decrease in cholinergic activity can increase levels of A $\beta$  peptides, creating a cycle of cholinergic loss, increased A $\beta$  production, and cognitive impairment (Strandridge JB, 2006). In this study, we wanted to investigate if depriving the hippocampus of cholinergic input would lead to increased levels of A $\beta$  peptide, in a mouse model in which rodent A $\beta$  has been replaced by knocked-in human A $\beta$ , but with APP being under the control of the natural promoter (Reaume AG et al, 1996).

### **1.1.1 Amyloid precursor protein (APP) and the production of A $\beta$ : amyloidogenic and non-amyloidogenic pathways.**

Amyloid plaques are composed mainly of a 4.5 kDa peptide termed amyloid- $\beta$  (A $\beta$ ) peptide (Selkoe, 2005). A $\beta$  peptide is released from the larger amyloid- $\beta$  precursor protein (APP), which has been identified as three major isoforms: APP<sub>695</sub>, APP<sub>751</sub>, and APP<sub>770</sub> (Buxbaum JD et al, 1992). In humans, the APP gene is located on chromosome 21 (Haass C and Selkoe DJ, 1993).

The physiological functions of APP are not known for certain, but likely include functioning as a growth factor or playing a role in cell survival (Beeson JG et al, 1994). Under physiological conditions, APP undergoes metabolic processing via a pathway that precludes A $\beta$  formation. In this “non-amyloidogenic” pathway, an enzyme called  $\alpha$ -secretase cleaves APP within the A $\beta$  sequence, resulting in the release of the secreted 90-100kDa N-terminus domain of the protein (also known as sAPP $\alpha$ ) into the extracellular space (Buxbaum JD et al, 1992; Vassar R et al, 1999). sAPP $\alpha$  is thought to be involved in neuroprotection and it has been implicated in neurite extension (Wallace WC et al, 1995). Alternate processing of APP occurs via the “amyloidogenic pathway”. This metabolic pathway requires activities of enzymes called  $\beta$ -secretase (Vassar R et al, 1999) and  $\gamma$ -secretase (Kimberly WT et al, 2003). Firstly, the  $\beta$ -secretase cleaves APP at the N-terminus of the A $\beta$  sequence, releasing a slightly shorter form of the secreted APP N-terminus fragment (sAPP $\beta$ ). Subsequent cleavage of the APP C-terminus fragment occurs, involving  $\gamma$ -secretase (a complex comprised of presenilin, nicastrin, Aph-1, and Pen-2), upon which A $\beta$  peptide is liberated and secreted into the extracellular space where it can aggregate into amyloid plaques (Kimberly WT et al, 2003). The two predominant forms of A $\beta$  are either 40 or 42 amino acids in length. A $\beta$ 42 is the more toxic of the two species and more apt

to aggregate. The two additional amino acids on the A $\beta$ 42 species are thought to increase its hydrophobicity and make it more prone to aggregation, compared to A $\beta$ 40 (Gouras GK et al, 2005).

A $\beta$  is secreted in a soluble state, polymerizing to form monomers, dimers, trimers and larger oligomers (Linder MD et al, 2006). High concentrations of soluble A $\beta$  are harmful to neurons. For example, altered synaptic morphology was associated with increased intraneuronal A $\beta$  levels (Tseng BP et al, 2004), and A $\beta$  can inhibit neuronal long-term potentiation, which serves as a correlate of memory function (Walsh DM et al, 2002). One proposed mechanism for soluble A $\beta$ 's deleterious effects on long term potentiation is that soluble A $\beta$  oligomers perturb normal expression of a synaptic immediate early gene which is required for memory formation (Lacor et al, 2004). Higher levels of soluble A $\beta$  are associated with greater synaptic loss (Lindner MD et al, 2006), and cognitive decline (Naslund J et al., 2000) in AD. Furthermore, increased soluble A $\beta$  levels also correlate with greater degree of AD severity (McLean CA et al, 1999).

After A $\beta$  oligomers aggregated into protofibrils, and insoluble A $\beta$  fibrils are formed, a dense  $\beta$ -pleated sheet of A $\beta$  becomes the core of extracellular plaques. It has been suggested that fibrillar A $\beta$  can also cause neuronal death by altering calcium homeostasis, increasing levels of oxidative stress, and disrupting neuronal synapses (Lahiri DK et al, 2007).

### **1.1.2 Anatomy of the cholinergic system**

Acetylcholine is a neurotransmitter implicated in a variety of functions, including cognition, regulation of arousal and sleep-wake cycle and selective attention (De LaCalle S et al, 1994).

The basal forebrain cholinergic system consists of the nucleus basalis of Meynert, the medial septal nucleus, and the horizontal and vertical diagonal bands of Broca (Auld DS et al, 2002). The septal complex is further divided into four sections: lateral, medial, ventral and posterior. The medial septal area is divided into the medial septum nucleus (which is located dorsally) and the ventrally located nucleus of the diagonal band of Broca. The nucleus of the diagonal band of Broca is subdivided into vertical and horizontal limbs (González I et al, 2007).

The hippocampus receives the majority of its cholinergic input from neurons which originate in the medial septal nucleus and the vertical limb of the diagonal band of Broca (Mesulam M, 2004). These large cholinergic neurons send their axonal projections to hippocampus via the fimbria fornix bundle (Wainer BH et al, 1985). These fibers terminate in all areas of hippocampus, but the densest projections are to supra and infragranular regions of dentate gyrus, the stratum oriens, and the stratum radiatum (Amaral DG and Kurz J, 1985). Retrograde labeling studies in rats indicate that very few medial septum and diagonal band neurons innervate frontal or parietal cortices (McKinney M et al, 1983).

The cerebral cortex and amygdala are innervated by the more caudally located portion of basal forebrain, the nucleus basalis of Meynert (Levey AI et al, 1987; Mesulam M, 2004). In rodents however, the cortex also contains cholinergic interneurons, which contribute 30% of the total cortical cholinergic innervation (Mesulam M, 2004). The areas of basal forebrain which contain cholinergic projection neurons receive significant input primarily from prefrontal cortex, as well as from piriform and insular cortices (Zaborszky L et al, 1997). The nucleus basalis complex receives cortical input via limbic areas, although it projects to all areas of cortex (Mesulam M, 2004). The horizontal limb of the diagonal band of Broca innervates cingulate cortex and visual cortex (McKinney M et al, 1983).

### **1.1.3 Biochemistry of the cholinergic system**

Cholinergic neurons contain the acetylcholine synthesizing enzyme, choline acetyltransferase (ChAT) (Mesulam M, 2004). ChAT is involved in the reaction which transfers the acetyl group from acetyl coenzyme A to choline, resulting in formation of acetylcholine (Oda Y, 1999). This reaction occurs at the axon terminal of cholinergic neurons; ChAT itself is synthesized in the perikaryon and is transported to the synapse via anterograde axonal transport (Oda Y, 1999). The acetylcholine degrading enzyme, acetylcholinesterase (AChE) is present on both the presynaptic and post-synaptic membranes of the cholinergic synapse; the surrounding glia contain butyrylcholinesterase (BChE) (Greig NH et al, 2005; Mesulam M, 2004). AChE hydrolyzes acetylcholine upon its release from synaptic vesicles into the synaptic cleft and choline is taken up by the presynaptic bouton (Ribeiro FM et al, 2006). High affinity choline uptake (HACU) is the rate limiting step in acetylcholine synthesis *in vivo* (Lapchak PA et al, 1991).

### **1.1.4 Animal models of cholinergic dysfunction**

It is possible to disrupt the cholinergic system by mechanically damaging cholinergic pathways, producing excitotoxic lesions of basal forebrain structures, or by using cholinergic antagonists at the cholinergic receptor. The loss of cholinergic neurons results in decreased acetylcholine levels in cortex as well as in other projection areas (Buxbaum JD et al, 1992). Lesioning the fimbria fornix causes both degeneration of cholinergic neurons in medial septum and significantly decreased levels of cholinergic enzyme activity in hippocampus (Beeson JG et al, 1994). Bilateral fimbria fornix lesions in rats decreased ChAT activity in hippocampus as early as one day following surgery. Three weeks following the lesion procedure, ChAT activity in the

hippocampus was still reduced, although ChAT activity in medial septum and diagonal band of Broca returned to normal levels (Häge B et al, 1996). Complete fimbria fornix lesions resulted in loss of AChE staining throughout the hippocampus (Lapchak PA et al, 1991; Lewis PR et al, 1967). However, lesions of the basal forebrain cholinergic system do not cause a complete depletion of ChAT in cortex or hippocampus owing to the presence of cholinergic interneurons in the cortex (Blaker SN et al, 1988). Previous work has shown that following fimbria fornix lesion, residual cholinergic fibers remain in layers I and III of presubiculum and in the molecular layer of hippocampus and subiculum (Blaker SN et al, 1988).

### **1.1.5 Cholinergic deficits in Alzheimer's Disease**

Multiple neurotransmitter systems are affected in AD, including cholinergic, adrenergic, dopaminergic and serotonergic (DeKosky ST et al, 2004). However, the most severe neurotransmitter dysfunction that occurs in AD is believed to involve dysfunction and subsequent loss of the basal forebrain cholinergic neurons (Hellström-Lindahl E, 2000; Liskowsky W and Schliebs R, 2006). Diminished cholinergic enzyme activity (i.e. ChAT and AChE) has been reported in AD brains (DeKosky ST et al., 1985) and ChAT mRNA levels are decreased in temporal, frontal, and parietal cortices in AD brains (Auld DS et al, 2002). AD patients have a decreased number of synaptic contacts in frontal cortex, compared to controls (Scheff SW et al, 1990) and this synapse loss correlates with cognitive decline (DeKosky ST and Scheff SW, 1990; Terry RD et al, 1991). Basal forebrain cholinergic neurons are differentially affected during the course of AD. For example, neurons in the posterior nucleus basalis are more vulnerable to degeneration compared to neurons in the medial septal/ diagonal band complex (DeKosky ST et al, 2002).

### 1.1.6 Relationship between cholinergic neurotransmission and APP processing

Many studies indicate that there is a relationship between perturbed cholinergic innervation and altered APP metabolism. In addition to lowering cholinergic enzyme levels, another effect of lesioning cortical-projecting cholinergic neurons in animals was upregulation of APP in cortex (Wallace WC et al, 1995), and a significant increase in sAPP $\beta$  in CSF (Haroutunian V et al, 1997). Cutting the fimbria fornix in rats also resulted in greater APP immunoreactivity in hippocampus four weeks following the lesion (Beeson JG et al, 1994; Lin L et al, 1999).

Pharmacological studies suggest that cholinergic neurotransmission “favors” non-amyloidogenic processing of APP. Chronic treatment with the muscarinic cholinergic receptor antagonist scopolamine resulted in lower activity of  $\alpha$ -secretase in the cortex (Liskowsky W and Schliebs R, 2006). Additionally, scopolamine treatment of APP- overexpressing mice led to increased levels of fibrillar A $\beta$ 1-40 and A $\beta$ 1-42 peptides (Liskowsky W and Schliebs R, 2006). Muscarinic receptor activation leads to increased secretion of APP $\alpha$  which results in decreased A $\beta$  levels (Lin L et al, 1999). Low doses of nicotine also favor the non-amyloidogenic pathway of APP metabolism (Schliebs R and Arendt T, 2006). Chronic treatment of mutant APP- overexpressing mice (Tg2576) with nicotine reduces plaque deposition (Schliebs R and Arendt T, 2006) and nicotine has been reported to prevent development of cellular toxicity induced by A $\beta$  peptides (Terry AV and Buccafusco JJ, 2003).

Some studies have shown that  $\beta$ -amyloid increases AChE and AChE has been shown to co-localize with  $\beta$ -amyloid plaques in Alzheimer brains (Lüth HJ et al, 2003; Schliebs R and Arendt T, 2006). This  $\beta$ -amyloid induced enhancement of AChE occurs via the  $\alpha$ 7nAChR (Schliebs R and Arendt T, 2006). In vitro studies have shown that AChE inhibitors increase the secretion of sAPP $\alpha$  in rat brain slices and cell culture (Liskowsky W and Schliebs R, 2006).

Additionally, *in vitro* studies indicate that AChE increases aggregation of  $\beta$ -amyloid by forming complexes with the fibrils (Liskowsky W and Schliebs R, 2006). The interaction between AChE and  $\beta$ -amyloid causes changes in the enzyme properties and results in increased neurotoxicity of  $\beta$ -amyloid fibrils (Liskowsky W and Schliebs R, 2006). Double transgenic mice that overexpress human AChE and APP have larger plaques and earlier plaque formation compared to APP overexpressing mice (Liskowsky W and Schliebs R, 2006).

APP metabolism is affected by cholinesterase inhibitor treatment, shifting it towards the non-amyloidogenic pathway (Zimmermann M et al, 2005). Cholinesterase inhibitors have been shown to effect APP metabolism *in vitro* by activating cholinergic receptors (Zimmerman M et al, 2005). *In vitro* studies have also shown that treatment of cells with AChE inhibitors lowers levels of soluble A $\beta$ 40 and soluble A $\beta$ 42 (Pakaski and Kasa, 2003) and increase secretion of sAPP $\alpha$  in cortical rat brain slices and cell culture (Schliebs R and Arendt T, 2006). BChE inhibitors increase brain acetylcholine levels and decrease levels of both A $\beta$ 40 and A $\beta$ 42 in transgenic mice (Greig NH et al, 2005). In addition, post-mortem studies have shown that patients with dementia with Lewy bodies that were treated with cholinesterase inhibitors had less cortical A $\beta$  deposits compared to non-treated patients (Ballard CG et al, 2007).

However, there may also be a reciprocal relationship between cholinergic stimulation and APP processing. *In vitro*, A $\beta$  exerts an inhibitory effect on acetylcholine release, by reducing both ChAT activity and pyruvate dehydrogenase (a precursor of acetyl coenzyme A), suggesting that A $\beta$  decreases acetylcholine release by modulating acetylcholine synthesis (Kar S et al, 2004). Injections of A $\beta$ 1-40 protein into the retrosplenial cortex of adult rats results in decreases in the number of M1 and M2 type muscarinic acetylcholine receptors in medial septum and horizontal limb of diagonal band of Broca (González I et al, 2007).

The results of these studies, taken together, imply that decreased cholinergic stimulation can increase formation of A $\beta$ . This A $\beta$ , in turn, generates conditions which are favorable for its release. In AD, this cycle might result in increased A $\beta$  formation, along with increased cholinergic deficits (Auld DS et al, 1998).

### **1.1.7 Cholinergic dysfunction in mouse models of AD**

Transgenic mouse models of AD exhibit cholinergic system dysfunction. Aged APP overexpressing (Tg2576) mice exhibit degeneration of ChAT-immunoreactive fibers in areas of A $\beta$  plaque deposition (Klinger M et al, 2003) and cognitive deficits correlate with soluble A $\beta$  levels in these animals (Lindner MD et al, 2006). Aged Tg2576 mice also have significantly decreased [ $^3$ H]HCh-3 binding (which measures high-affinity choline uptake) in cortex, indicating a loss of cholinergic terminals (Klinger M et al, 2003). In young adult Tg2576 mice, there was a reduction in [ $^3$ H]HCh-3 binding in anterior cortical areas, compared to wildtype mice, although these young animals did not show cholinergic fiber degeneration, suggesting that the functional changes precede structural losses (Klinger M et al, 2003). Tg2576 mice exhibit reduced binding of M1-muscarinic acetylcholine receptors compared to wildtypes (Apelt J et al, 2002). This reduction in binding is seen by 8 months of age, before cortical plaque deposition (but following production of soluble A $\beta$ ) and remains low to at least 17 months of age (Apelt J et al, 2002). There is no difference in the number of basal forebrain cholinergic neurons between Tg2576 mice and wildtypes, at any of the ages examined, nor was there a difference in ChAT or AChE activity (Apelt J et al, 2002).

APP/PS1 transgenic mice exhibit a reduction in size and density of cholinergic synapses in hippocampus and frontal cortex (Wong TP et al, 1999). Compared with aged-matched

controls, PDAPP mice (another transgenic APP overexpressing strain) have more than a 50% decrease in cholinergic nerve terminal varicosities (German DC et al, 2003). The most dramatic loss of cholinergic nerve terminals in PDAPP mice occurred between 2 and 4 months, before the onset of A $\beta$  plaque deposition (German DC et al, 2003). However, despite the early changes in number of ChAT varicosities, there was no decrease in the number of cholinergic basal forebrain neurons in aged PDAPP mice (German DC et al, 2003).

### **1.1.8 Fimbria fornix lesioned humanized A $\beta$ mouse: cholinergic-amyloid interactions**

*In vivo* investigations of the effect of fimbria-fornix lesion on A $\beta$  production have been hampered by species-specific differences in the A $\beta$  peptide, as rodents have a different A $\beta$  sequence than humans. A few recent studies attempted to overcome this problem by employing transgenic mice that over-express human APP. van Groen et al reported that 11 months following fimbria fornix lesion there was no difference in the number of A $\beta$  plaques in the hippocampus (van Groen et al, 2003). Another study in APP/PS-1 mice also showed that fimbria fornix lesion did not affect hippocampal APP levels or A $\beta$  production (Liu L et al, 2002). Treatment with an  $\alpha$ 7nAChR agonist in APP/PS1 mice following fimbria fornix lesions results in decreased size of cholinergic neurons, unlike wild-type mice which show no change in neuronal size following treatment (Ren K et al, 2007).

However, the transgenic APP and APP/PS-1 mice used in these studies continuously overexpress the APP gene and overproduce A $\beta$  which accumulates in plaques (Kurt MA et al, 2001). This makes it difficult to study more subtle changes in APP processing and A $\beta$  production following cholinergic lesions. The animal model we used in our study is a unique “humanized”

A $\beta$  (hA $\beta$ ) mouse model of AD (see Methods). Unless there is an additional PS1 mutation, these mice do not deposit A $\beta$  plaques spontaneously (Flood DG et al, 2002).

This study is the first to employ a non-transgenic hA $\beta$  mouse model to examine the association between the altered cholinergic neurotransmission and amyloidogenic APP metabolism. The results presented here will provide better understanding of this interaction and will help in the development of improved therapies for AD.

## 2.0 METHODS

### 2.1.1 Humanized A $\beta$ mice

Adult APP<sup>NLh/NLh</sup> mice were used in this study. These mice have an A $\beta$  sequence which is analogous to human and contain the Swedish APP mutation (FADK670N/M671L), but unlike APP/PS1 mice they have normal APP expression under an endogenous promoter (Reaume AG et al, 1996). Therefore, these mice produce human A $\beta$  without APP overexpression. Mice had ad libitum access to food and water. The University of Pittsburgh Institutional Animal Care and Use Committee approved all procedures.

### 2.1.2 Fimbria fornix lesion

APP<sup>NLh/NLh</sup> mice were anesthetized with 4.6ml/kg of Equithesin and placed in Kopf stereotaxic device adapted for mice. Scalp was cut to expose the skull and craniotomy performed. A 1mm hook was lowered and a 3.0mm cut was made (AP +0.7mm to -2.3mm from Bregma, ML 0.5mm from midline, DV -3.8mm). The hook was slowly extracted from the brain and the procedure was repeated on the contralateral side (adapted from Liu L et al, 2002). Surgical controls underwent similar procedure, with corpus callosum being lesioned instead of fimbria fornix. Coordinates used for control surgery were: (from Bregma, AP +1.7mm to -0.6mm, ML 0.5mm, DV 2.0mm) (adapted from Ginsberg SD and Martin LJ, 1998). Following lesion procedures,

bone wax was placed on the edges of the skull and the wound was sutured. Animals remained under observation; after regaining spontaneous movement they were returned to mouse room and allowed to recover for 2.5 weeks. At designated timepoints post-lesion, mice were overdosed with equithesin and perfused transcardially with phosphate buffer. The brain was removed and blocked approximately 1mm caudal to the optic chiasm. The rostral portion of brain was immersion fixed in 4% paraformaldehyde overnight, then cryoprotected (immersed in 15% sucrose solution overnight, followed by immersion in 30% sucrose solution), and 40µm thick sections were cut using a cryostat. The cut sections were stored in cryoprotectant until further processing for histology and immunocytochemistry. Hippocampi from the remaining caudal portion of the brain were dissected out and frozen at -80°C.

### **2.1.3 Nissl Stain**

Slide mounted tissue sections were dehydrated in graded ethanols, from 50% ethanol to 100% ethanol, then rehydrated in series of alcohols (from 100% ethanol to 50% ethanol) and dH<sub>2</sub>O. Slides were placed in Cresyl violet solution (500mL dH<sub>2</sub>O, 1.5mL glacial acetic acid, 2.5g Cresyl violet acetate) for 45 sec. Sections were dipped in dH<sub>2</sub>O, then placed in dH<sub>2</sub>O for one minute. This was followed by one minute in 50% ethanol, 70% ethanol, 95% ethanol, and 2 minutes in 100% ethanol. Tissue was then cleared in xylenes and coverslipped with Permount.

### **2.1.4 Luxol Fast Blue**

Slide mounted tissue sections were dehydrated in series of alcohols from 50% ethanol to 95% ethanol. Slides were placed in 0.1% Luxol Fast Blue solution (100mL 95% ethanol, 0.5ml glacial

acetic acid, 0.1g Luxol Fast Blue) for 5 minutes. Slides were dipped in 95% ethanol, then differentiated first in 0.05% lithium carbonate solution, followed by 70% ethanol, for 30 seconds each. Sections were dehydrated in series of graded alcohols (from 70% ethanol to 100% ethanol), cleared in xylenes and coverslipped using Permount.

### **2.1.5 AChE Histochemistry**

Free floating mouse tissue sections were rinsed in 0.1M phosphate buffer (pH 7.4) three times, for five minutes each time, followed by rinse in 0.1M sodium acetate buffer (pH 6.0) for 15 minutes. Sections were incubated in AChE solution (65mL of 0.1M sodium acetate buffer, 50mg acetylthiocholine iodide, 5mL 0.1M sodium citrate buffer, 10mL 0.03M cupric sulfate, 15mL dH<sub>2</sub>O, 4mL 0.5M potassium fericyanide and 1mL 1mM tetraisopropyl pyrophosphoramidate) for 60 minutes at room temperature, in the dark. Sections were rinsed in 0.1M sodium acetate buffer (pH 6.0) five times, for three minutes each time. Sections were placed in 4% ammonium sulfide for 1 minute, followed by eight rinses, five minutes each, in 0.1M sodium nitrate buffer. Staining reaction was enhanced by incubating sections in 0.1% silver nitrate for 45 seconds. This was followed by five rinses in 0.1M sodium nitrate buffer, for three minutes each time. Sections were mounted on gelatin-coated slides and allowed to air dry. Slides were dehydrated through series of graded alcohols (from 50% ethanol to 100% ethanol), cleared in xylenes and coverslipped using Permount.

### **2.1.6 ChAT Immunocytochemistry**

Free floating mouse tissue sections were rinsed in 0.1M phosphate buffer (pH 7.4). Sections were incubated in 3% rabbit serum in TBST (0.1M Trizma Base, 9g NaCl, 0.25% Triton-X 100, pH 7.4) for 30 minutes. Tissue sections were rinsed two times, for ten minutes each time in 1% rabbit serum in TBST, then incubated in primary antibody (anti-ChAT, 1:100, Chemicon) in 1% rabbit serum in TBST for 4 nights at 4°. Following incubation in primary antibody, tissue was rinsed in 1% rabbit serum in TBST two times, for ten minutes each time, then treated with biotinylated rabbit anti-goat secondary antibody (1:250, American Qualex) in 1% rabbit serum in TBST for 60 minutes at room temperature. This was followed by three rinses in TBST, for 5 minutes each, and then a one hour incubation in avidin-biotin solution (ABC Kit, Vector Labs) made in TBST. Following ABC incubation, tissue sections were rinsed three times, five minutes each in TBST. This was followed by additional rinses (three rinses, five minutes each time) in imidazole acetate buffer (0.082M sodium acetate and 0.01M imidazole), pH 7.4. Reaction was visualized using DAB (3,3'-Diaminobenzidine tetrahydrochloride) in imidazole acetate buffer with 2.5% nickel ammonium sulfate and 0.3% H<sub>2</sub>O<sub>2</sub>. Sections were mounted on gelatin-coated slides and allowed to air dry. Slides were dehydrated through series of graded alcohols (50% ethanol to 100% ethanol), cleared in xylenes and coverslipped using Permount.

### **2.1.7 Analysis of ChAT-immunoreactive fiber density**

40x images were taken throughout molecular layer (six images, three from each hemisphere) and CA3 (six images, three from each hemisphere) of six fimbria-fornix lesioned mice, three surgical controls and five naïve mice. The density of fibers was assessed by applying stereological

principles as described previously. A cycloid grid was overlaid on the images and numbers of intersections between ChAT fibers and the cycloids were counted in every image (Ikonomic MD et al, 2007). The counts for every image for each region were then averaged together for each animal.

### **2.1.8 AChE Activity Assay**

Hippocampi from nine fimbria-fornix lesioned mice, five surgical controls and eleven naïve animals were assessed for cholinergic denervation by an AChE activity assay. The AChE activity assay is a colorimetric assay based on the principle that AChE hydrolyzes acetylthiocholine (an analog of the natural substrate) to produce thiocholine and acetate; the assay measures the rate of production of the thiocholine. The resulting thiocholine reacts with DTNB to produce 5-thio-2-nitro-benzoic acid (a yellow anion) and the rate of color production is then measured using a plate reader set at a wavelength of 410nm.

Frozen hippocampi were weighed, sonicated in 1x phosphate buffered saline, then homogenized in buffer containing 10mM disodium EDTA and 0.5% Triton X-100, in dH<sub>2</sub>O. In 96-well plates, 5µl of homogenized tissue samples or blanks (only containing homogenizing buffer containing 10mM disodium EDTA and 0.5% Triton X-100 in dH<sub>2</sub>O) were pipetted, in triplicate, into wells. 175µl of reaction mix [50mM sodium phosphate buffer, 3.3mM 5,5'-dithiobis-(2-nitrobenzoic acid) (DTNB) and 0.75mM tetraisopropylpyrophosphoramidate (ISO-OMPA)] was added to each well. Optical density (OD) readings were taken at 410nm wavelength. The plate was then covered and incubated at 37° for 30 minutes. The plate was removed from the oven and 20µl of substrate [5 mM acetylthiocholine (AThCh)] added to each well. The plate was then covered and incubated for an additional 30 minutes at 37°. Final OD

reading was taken immediately upon removal from oven, using plate reader set at 410nm wavelength. The results were read at time of the linear portion of the enzyme kinetic curve.

The net change in absorbance was determined by subtracting the final OD reading from the initial OD reading of each sample. The change in OD of the blanks was calculated and averaged. The final change in absorbance was calculated by subtracting the average of the blanks from every sample. Protein levels ( $\mu\text{g} / \mu\text{l}$ ) were determined using the BCA protein assay (described below) and the final AChE activity for each sample was calculated by using the following formula (Ellman GL et al, 1961):

$$\text{ENZYME RATE} = \frac{(\Delta \text{Absorbance}) (\text{Reaction Volume})}{(\epsilon) (\text{Sample Conc.}) (\text{Sample Vol.}) (\text{Incubation Time})}$$

$$\text{Extinction Coefficient } (\epsilon) \text{ of DNTB} = 13.6 \times 10^3 \text{ Molar} = 13.6 \text{ mmol} / \mu\text{l}$$

$$\text{RATE OF} = \frac{(\text{Net } \Delta \text{OD}_{410}) (200 \mu\text{l}) (60 \text{ min/hr})}{(13.6 \text{ nmol}/\mu\text{l}) (\mu\text{g}/\mu\text{l}) (\mu\text{l}) (30 \text{ min})} = \text{mmol} / \text{hr} / \mu\text{g}$$

$$\text{HYDROLYSIS} = \frac{(\text{Net } \Delta \text{OD}_{410}) (29.41)}{(\mu\text{g})}$$

$$\text{ACHE} = \frac{(\text{Net } \Delta \text{OD}_{410}) (29.41)}{(\mu\text{g})} = \text{mmol} / \text{hr} / \text{g}$$

$$\text{ACTIVITY} = \frac{(\text{Net } \Delta \text{OD}_{410}) (29.41)}{(\mu\text{g})}$$

### 2.1.9 ChAT Activity Assay

ChAT activity was determined on nine fimbria fornix lesioned mice, five surgical controls and eleven naïve animals to determine the success of the fimbria fornix lesions in removing cholinergic input from hippocampus. The ChAT activity assay is a two-phase radiometric assay dependent on the fact that ChAT synthesizes acetylcholine. ChAT is an enzyme which reacts with acetyl Co-A and choline to produce acetylcholine and coenzyme-A.  $^{14}\text{C}$ -labeled acetyl Co-A is used in this assay. Following the reaction, any unreacted substrate remains in the aqueous phase and will not scintillate (water is not a scintillation solvent) (Fonnum, 1975). The product ( $^{14}\text{C}$ -Acetylcholine) is extracted into organic phase and counted.

Frozen hippocampi were weighed, sonicated in 1x phosphate buffered saline, then homogenized in buffer containing 10mM disodium EDTA and 0.5% Triton X-100, in  $\text{dH}_2\text{O}$ . The reaction was initiated by the addition of 5 $\mu\text{l}$  of sample or blanks (only homogenizing buffer containing 10mM disodium EDTA and 0.5% Triton X-100 in  $\text{dH}_2\text{O}$ ), in triplicate, to Eppendorf tubes containing 10 $\mu\text{l}$  of assay mixture [250 $\mu\text{l}$  of incubation buffer (100mM sodium phosphate buffer, 600mM sodium chloride, 20mM choline chloride and 10mM disodium EDTA), 250 $\mu\text{l}$  of  $^{14}\text{C}$  labeled substrate (0.4mM [ $^{14}\text{C}$ ]Acetyl Co-A {40-60 mCi/mmol}) and 5 $\mu\text{l}$  of 20mM eserine salicylate]. Tubes were incubated a water bath for 30 minutes at 37°C. Following incubation, tubes were taken out of the water bath, their lids removed, and tubes were placed into their corresponding scintillation vials. The reaction was stopped by adding 4ml of ice cold Reaction Rinse (10mM sodium phosphate) to the vials. This was followed by the addition of 1.6ml of aqueous extraction solution (acetonitrile and 5mg/ml tetraphenylboron) and 8ml of organic extraction fluid (Econofluor). Vials were tightly capped, mixed by inversion and cps were read 24 hours later. The results were read at time of linear portion of the enzyme kinetic curve.

The cpms of the blanks were averaged together and the cpms of the triplicates were averaged for every mouse. Each mouse average was subtracted from the blank average to obtain a net cpm reading for every sample. Protein levels ( $\mu\text{g} / \mu\text{l}$ ) were determined using a BCA protein assay (described below). Final ChAT activity was calculated by using the following formula:

$$\text{CHAT ACTIVITY} = \frac{(\text{Net cpm}) (0.11636)}{(\text{total } \mu\text{g})} = \mu\text{mol} / \text{hr} / \text{g}$$

#### 2.1.10 Soluble A $\beta$ 42 ELISA

Soluble A $\beta$ 42 ELISA was performed on hippocampi from nine fimbria fornix lesioned mice, five surgical controls and nine naïve mice. Two naïves which were included in the AChE and ChAT biochemical experiments were not included in the A $\beta$ 42 ELISA; it was determined that they were not accurately perfused and excess blood in the cerebrovasculature would affect A $\beta$ 42 ELISA outcomes.

Frozen hippocampi were weighed and sonicated in 1x phosphate buffered saline. Brain homogenates were sonicated briefly in A $\beta$  extraction buffer [1.5ml 0.4% DEA buffer (200 $\mu\text{l}$  DEA, 1ml 5M sodium chloride, dH $_2$ O), 15 $\mu\text{l}$  Sigma protease inhibitor, 37.5 $\mu\text{l}$  40mM AEBSF], then centrifuged for 60 minutes at 135,000 x g at 4°C, to extract soluble A $\beta$  peptides in the supernatant (the remaining pellet contained membrane-bound APP). Soluble A $\beta$ 42 ELISA was performed on homogenate supernatants using the A $\beta$ 1-42 Kit from Biosource (Carlsbad, CA). Standards were prepared according to manufacturer's instructions, as follows. The human A $\beta$ 42

standard was reconstituted to 1.0 $\mu$ g/ml with Standard Reconstitution Buffer (55 mM sodium bicarbonate, pH 9.0). The reconstituted standard was diluted serially into the provided Diluent Buffer to produce standards with final concentrations of: 1000pg/ml, 750 pg/ml, 500pg/ml, 250pg/ml, 125pg/ml, 62.5pg/ml, 31.3pg/ml, 15.6pg/ml and 0pg/ml. Supernatants were diluted (1:2) in Diluent Buffer containing 1mM AEBSF. 50 $\mu$ L of standards or samples/well, along with 50 $\mu$ l/well of detection antibody (rabbit anti-human A $\beta$ 42), were added to an ELISA plate coated with a capture antibody generated against the N-terminal portion of A $\beta$ . The plate was covered and incubated overnight at 4°C. The next day, the plate was rinsed multiple times with the provided Working Wash Buffer. Following rinses, anti-rabbit IgG-AP secondary antibody was prepared by adding 60 $\mu$ l of 100x concentrate anti-rabbit IgG-AP to 12ml of Secondary Antibody Diluent. 100 $\mu$ l of anti-rabbit IgG-AP was pipetted into each well and the plate incubated at room temperature for 30 minutes. During secondary antibody incubation, the Fluorescent Substrate Solution was prepared by adding 11ml of Alkaline Phosphatase Fluorescent Substrate Resuspension Buffer to 6.6mg of Alkaline Phosphatase Fluorescent Substrate. The plate was rinsed multiple times with Working Wash Buffer. Following rinses, 100 $\mu$ l of AP Fluorescent Substrate Solution was added to each well. The plate was incubated for 30 minutes in the dark, at room temperature, then read at a wavelength of 460nm. The standard curve was prepared by plotting the absorbance reading for each standard vs. its concentration (pg/ml). The triplicate samples were averaged and read against the standard curve, to determine A $\beta$  levels. Final A $\beta$  levels were normalized to protein levels (as determined by BCA Protein Assay, described below) and expressed as pg/mg.

### **2.1.11 BCA Protein Assay**

Protein assays on samples were completed following ChAT assay, AChE assay and soluble A $\beta$ 42 ELISA. The same aliquots used for each of those experiments were used in determining protein concentrations and making final adjustments to the data for each assay. Diluted albumin [BSA, 2.0mg/ml in 0.9% saline and 0.05% sodium azide, (Pierce #23209)] standards were prepared in distilled H<sub>2</sub>O (for proteins used in ChAT and AChE assay) or in 50mM Tris buffer, pH 6.8 (for proteins used in A $\beta$ 42 ELISA) at the following concentrations: 1500  $\mu$ g/ml, 1000  $\mu$ g/ml, 750  $\mu$ g/ml, 500  $\mu$ g/ml, 250  $\mu$ g/ml, 125  $\mu$ g/ml, and 0  $\mu$ g/ml. Working reagent was made by combining 20 mL of BCA Reagent A [containing sodium carbonate, sodium bicarbonate, bicinchoninic acid and sodium tartrate in 0.1M sodium hydroxide (Pierce #23228)] and 0.4 mL of BCA Reagent B [contains 4% cupric sulfate (Pierce #23224)]. 10 $\mu$ l of the standards and each homogenized sample, in triplicate, were pipetted into each well of a 96-well plate. This was followed by the addition of 200 $\mu$ l of working reagent to each well. The plate was covered, briefly vortexed and incubated for 30 minutes at 37°. The plate was removed from the oven and absorbance read using the plate reader set at 470nm wavelength. The standard curve was prepared by plotting the absorbance reading for each standard against its concentration ( $\mu$ g/ml). Triplicate sample values were averaged and measured on the standard curve, to determine final protein concentration.

### **2.1.12 Statistics**

The effects of fimbria-fornix lesion on ChAT immunoreactive fiber density, ChAT activity, AChE activity and soluble A $\beta$ 42 levels were analyzed by ANOVA, with post-hoc Bonferroni

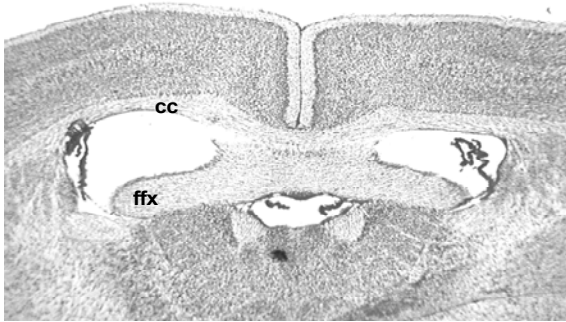
testing with GraphPad InStat 3.06 for Windows (San Diego, CA). Correlative analyses were determined by Pearson's correlation coefficient also using GraphPad InStat 3.06 for Windows. Outliers were identified using Grubbs' test for outliers. All values were expressed as means  $\pm$  SE.

## **3.0 RESULTS**

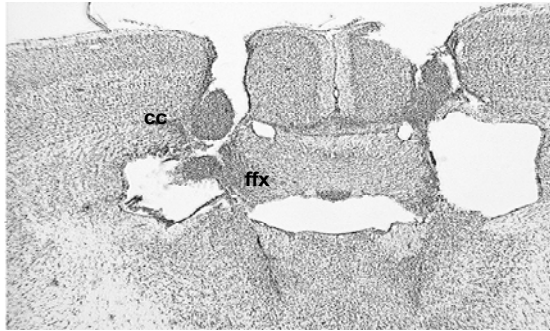
### **3.1.1 Histological verification of the fimbria fornix lesions**

Analysis of brain tissue sections processed for Nissl and Luxol Fast Blue staining confirmed bilateral transection of the fimbria-fornix in all fimbria fornix lesioned animals, while only minimal damage was detected to other structures, including cortex and thalamus (Figure 1B). In Nissl and Luxol Fast Blue stained tissue sections from the surgical control group, the corpus callosum was lesioned bilaterally, with minimal damage to other structures (Figure 1C) and with the fimbria fornix remaining intact (Figure 1D).

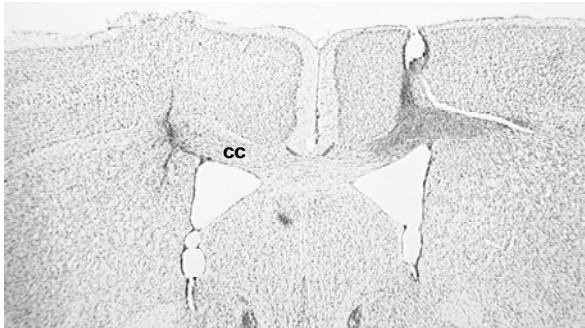
A. Naive



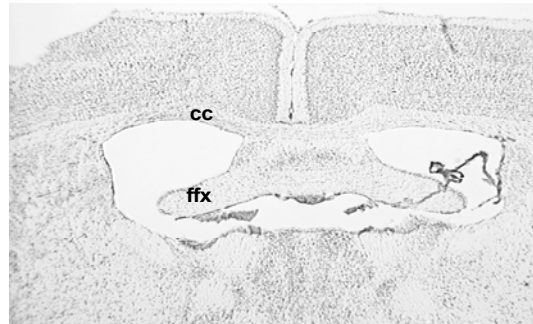
B. FFX lesion



C. Surgical Control



D. Surgical Control

**Figure 1 Histological proof of proper lesion placement.**

Nissl stained coronal sections through fimbria-fornix from naïve (A) and fimbria-fornix lesioned (B) mouse brain. Note that ffx is intact in naïve mouse, and substantially lesioned bilaterally in the ffx lesioned animal. C and D. Nissl stained coronal sections of surgical control mouse, at level of rostral corpus callosum (C) and fimbria-fornix (D). There is a bilateral lesion to cc (C), while ffx is intact (D) in the same animal. cc= corpus callosum; ffx= fimbria-fornix

**Table 1 Fimbria-fornix lesion results in decreased ChAT-ir fiber density in hippocampus**

	Naive	Fimbria fornix lesion	Surgical control	ANOVA
<b>DG</b>				
<b>Mean ± SE</b>	106.77 ± 12.81	65.08 ± 5.39	91.17 ± 8.41	F= 5.832
<b>Range</b>	74.33-145.50	46.5-80.67	77.5-106.5	P= 0.0188 <sup>1,2</sup>
<b>CA3</b>				
<b>Mean ± SE</b>	119.73 ± 13.19	69.64 ± 7.41	109.67 ± 4.86	F=7.878
<b>Range</b>	89-167.33	41.5-94.17	100.67-117.33	P=0.0075 <sup>1,2</sup>

<sup>1</sup> Naïve vs. fimbria-fornix lesion, p<.05

<sup>2</sup> Fimbria fornix lesion vs. surgical control, nonsignificant

### **3.1.2 Fimbria fornix lesion results in reduced densities of cholinergic fibers in the hippocampus: AchE histochemistry and ChAT immunocytochemistry**

AChE histostaining and ChAT immunocytochemistry are accepted as reliable markers of fimbria fornix lesion efficacy (Alonso JR et al, 1996). Analyses of AChE-histostained sections revealed a dense network of fibers throughout the hippocampus of naïve mice (and surgical controls). Compared to the naïve group, fimbria-fornix lesioned mice had decreased density of AChE stained fibers in the hippocampus; this was particularly evident in the molecular layer of dentate gyrus and in CA3 (Figure 2).

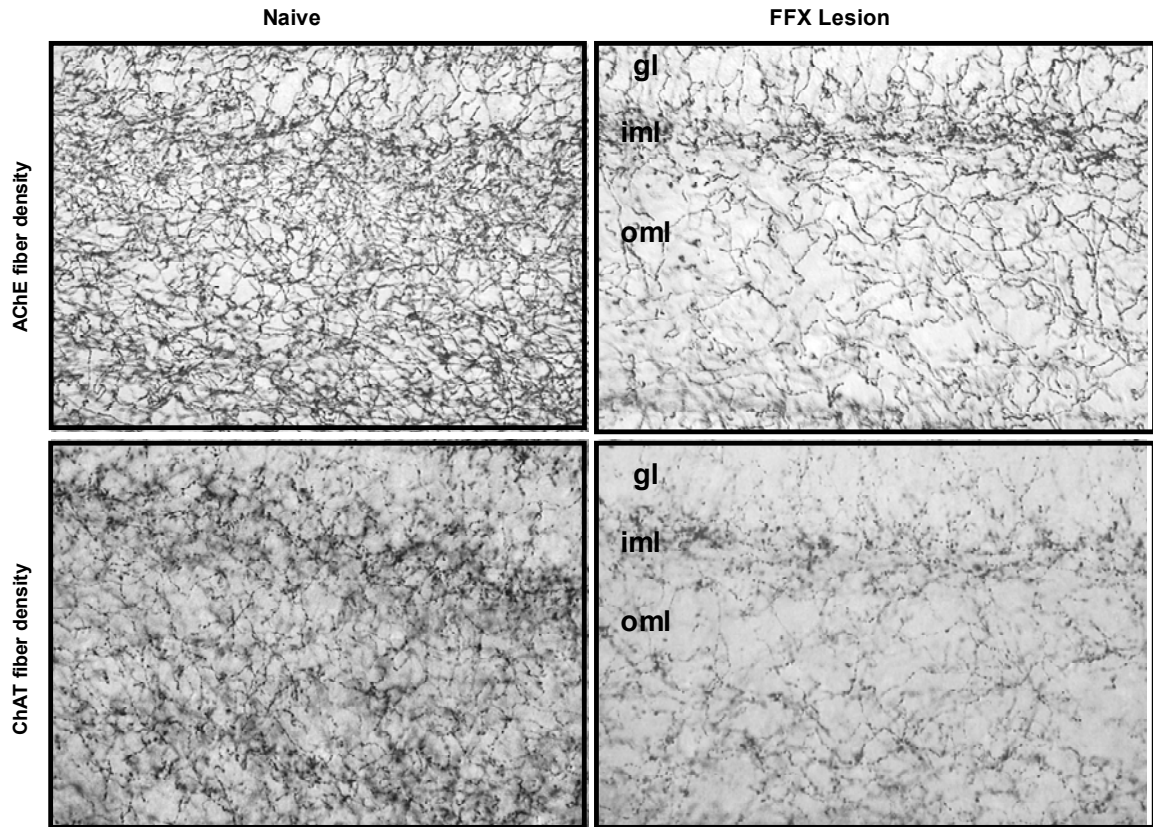


**Figure 2. Histochemical and immunohistochemical evidence of fimbria fornix lesion efficacy.**

**AChE-positive (upper row) and ChAT-immunoreactive (lower row) fibers in dentate gyrus have significantly lower density in fimbria fornix lesioned mice (right column) compared to naïves (left column). gl = granular cell layer of dentate gyrus; iml= inner molecular layer of dentate gyrus; oml= outer molecular layer of dentate gyrus**

Similar results were observed using ChAT immunocytochemistry. In naïve mice, ChAT immunocytochemical staining revealed a dense network of fibers throughout the hippocampus. The molecular layer of dentate gyrus and CA3 were chosen for analysis of changes in ChAT immunoreactive fiber density (Figure 3 and Table 1). The sections from fimbria -fornix lesioned animals had decreased fiber density in hippocampus compared to those from naïve animals and surgical controls. In the molecular layer of the dentate gyrus, there was a statistically significant ( $p < 0.05$ ) 39% decrease in ChAT-immunoreactive fibers following fimbria-fornix lesions compared to naïve animals. A non-significant 28.6% decrease in ChAT-immunoreactive fibers

was seen in the fimbria fornix lesioned group compared to surgical controls. No significant difference in ChAT-immunoreactive fiber densities was detected between surgical controls and the naïve group (Figure 3A).

In the CA3 region, there was a 41.8% decrease in the number of ChAT immunoreactive fibers in fimbria fornix lesioned mice compared to the naïve group ( $p < 0.05$ ; Figure 3B). A non-significant 36.5% reduction in CA3 ChAT-ir fibers was seen in fimbria fornix lesioned animals compared to surgical controls. There was no difference in ChAT fiber number in CA3 between surgical controls and naïve animals.

**Table 2 Fimbria fornix lesion results in decreased cholinergic enzyme activity and increased soluble A $\beta$ 42 levels**

	Naive	Fimbria fornix lesion	Surgical control	ANOVA
<b>AChE Activity (mmol/hr/g)</b>				
<b>Mean <math>\pm</math> SE</b>	1.16 $\pm$ 0.07	0.58 $\pm$ 0.05	1.04 $\pm$ 0.06	F= 23.96
<b>Range</b>	0.72-1.45	0.41-0.81	0.90-1.20	P< .0001 <sup>1,2</sup>
<b>ChAT Activity (<math>\mu</math>mol/hr/g)</b>				
<b>Mean <math>\pm</math> SE</b>	44.49 $\pm$ 2.12	22.55 $\pm$ 1.93	36.67 $\pm$ 2.49	F= 29.81
<b>Range</b>	32.83- 58.10	15.75-30.69	29.10-42.25	P<.0001 <sup>1,2</sup>
<b>Soluble A<math>\beta</math>42 (pg/mg)</b>				
<b>Mean <math>\pm</math> SE</b>	11.51 $\pm$ 3.68	38.88 $\pm$ 5.20	22.71 $\pm$ 3.63	F=10.66
<b>Range</b>	-0.26-30.68	19.58-72.53	9.65-31.85	P=.0007 <sup>1</sup>

<sup>1</sup> naïve vs. ffx lesion,  $p < .01$

<sup>2</sup> ffx lesion vs. surgical control,  $p < .01$

### 3.1.3 Fimbria fornix lesion results in loss of hippocampal AChE activity

Hippocampal AChE activity assay is a well established method of confirming a successful fimbria fornix lesion (Fuxe K et al, 1994). Our analysis was based on an AChE activity assay in hippocampal tissue homogenates from nine fimbria-fornix lesioned mice, five surgical controls,

and eleven naïve animals (Table 2 and Figure 4). Mice in the naïve group had a mean AChE activity of  $1.16 \pm 0.07$  mmol/hr/g. Following fimbria fornix lesion, the mean AChE activity was reduced to  $0.58 \pm 0.05$  mmol/hr/g. Surgical controls had a mean AChE activity of  $1.04 \pm 0.06$  mmol/hr/g.

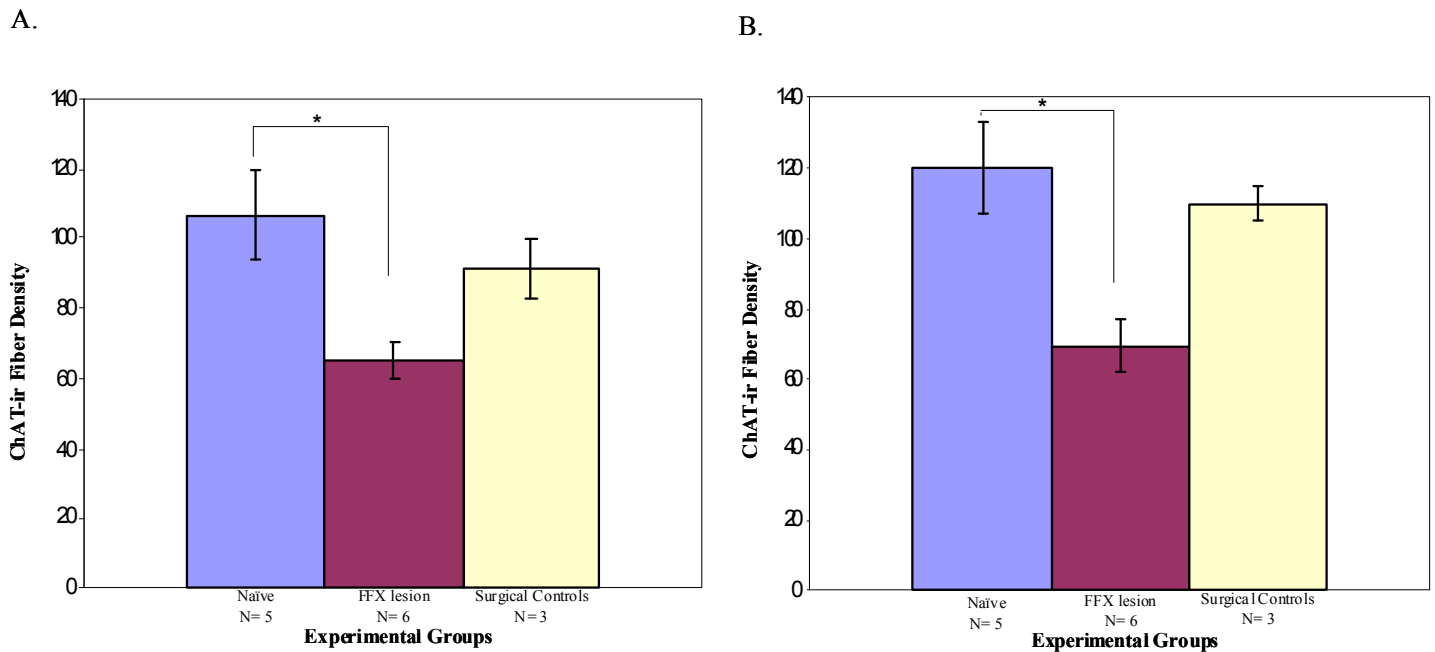


**Figure 3** The effect of fimbria fornix lesion on ChAT-immunoreactive fiber density in the dentate molecular layer (A) and CA3 (B) of hippocampus. A. In fimbria fornix lesioned animals, there is a significant reduction of ChAT immunoreactive fiber density in molecular layer of dentate gyrus when compared to naïve mice. B. A similar reduction in ChAT immunoreactive fiber density was observed in CA3 region of hippocampus in fimbria fornix lesioned mice compared to naïve mice. \*  $p < .05$

There was a statistically significant decrease ( $p < 0.01$ ) in hippocampal AChE activity in fimbria fornix lesioned animals compared to both naïves and surgical controls (Figure 4). In the fimbria fornix lesioned mice, AChE activity was decreased by 50.1% and 44.2% compared to naïves and surgical controls, respectively. AChE activity levels in surgical controls and naïve mice were not different.

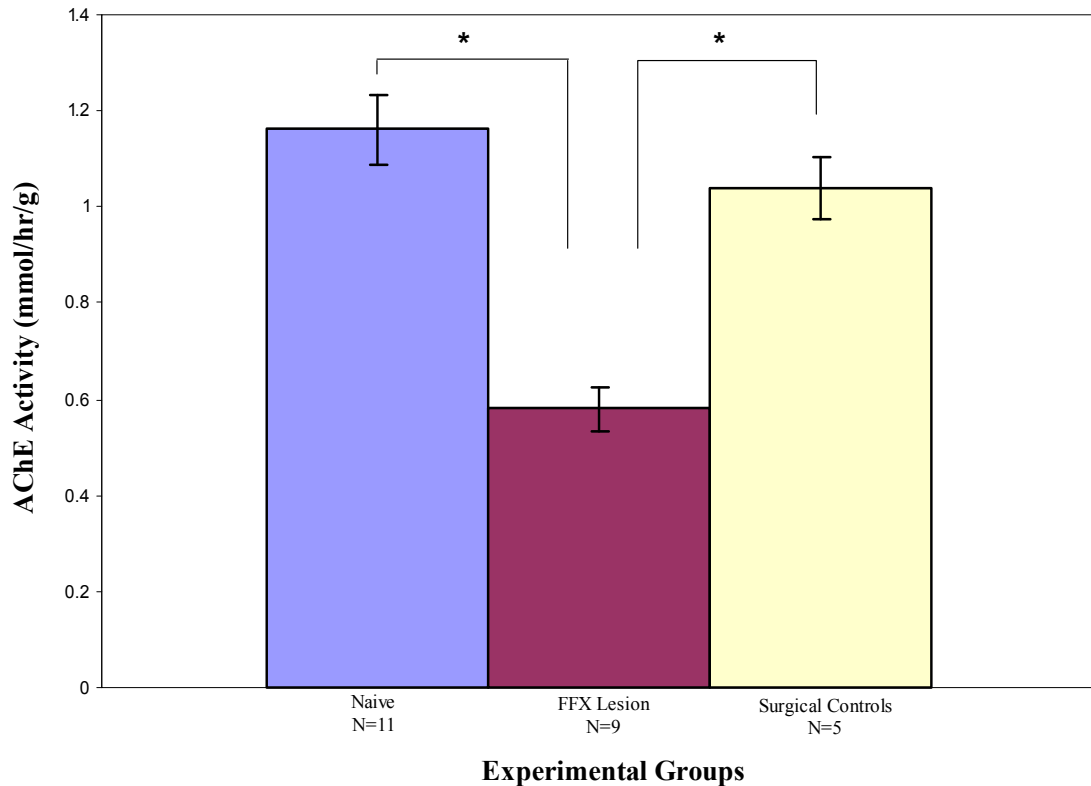


**Figure 4. The effect of fimbria fornix lesion on AChE activity in hippocampus. Bilateral fimbria fornix lesion results in a significant decrease in AChE activity in hippocampus compared to both naïve mice and surgical control groups. \*  $p < .01$**

### **3.1.4 Fimbria fornix lesion results in loss of hippocampal ChAT activity**

Hippocampal ChAT activity assay is another well established method of confirming a successful fimbria fornix lesion (Fuxe K et al, 1994). ChAT activity was analyzed in the hippocampus from nine fimbria fornix lesioned mice, five surgical control mice, and from eleven naïve mice (Table 2 and Figure 5). In the naïve group of mice, the mean ChAT activity was  $44.49 \pm 1.93 \mu\text{mol/hr/g}$ . Post-lesion, mean ChAT activity in hippocampus was  $22.55 \pm 2.12 \mu\text{mol/hr/g}$ . Surgical control mice had an average ChAT activity of  $36.67 \pm 2.49 \mu\text{mol/hr/g}$ .

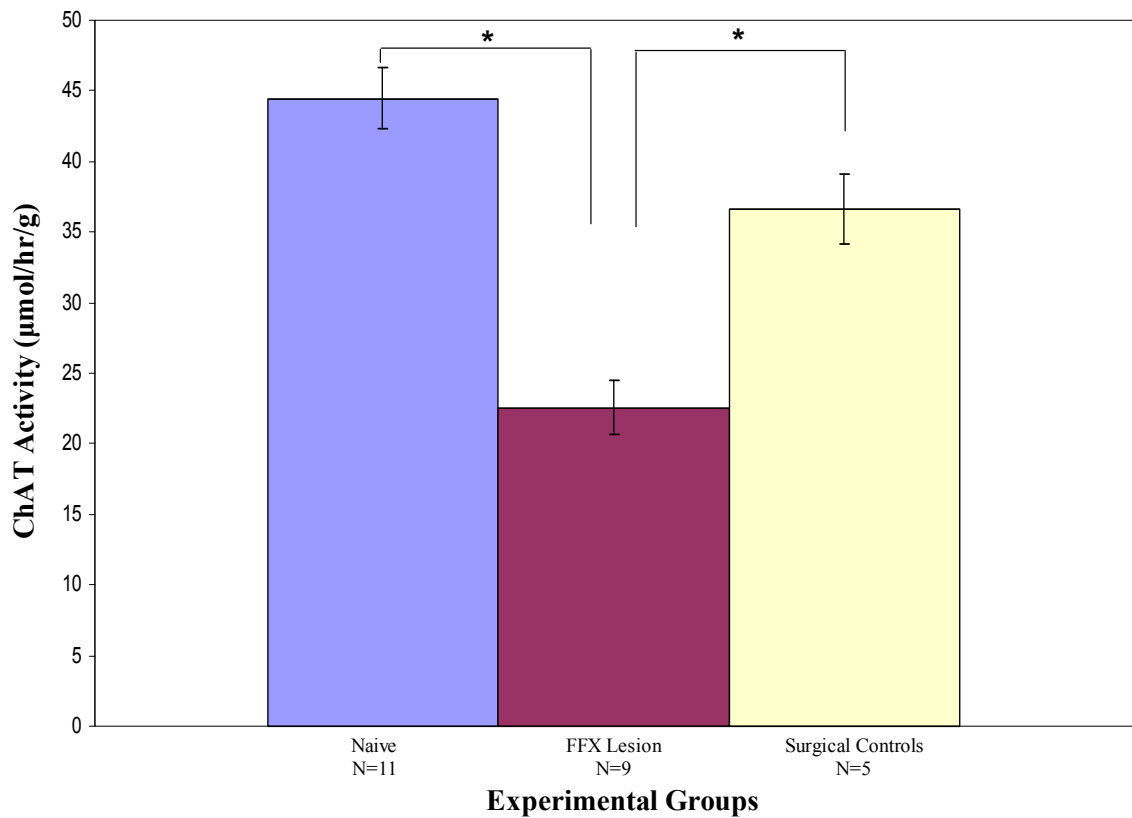


**Figure 5. The effect of fimbria fornix lesions on ChAT activity in hippocampus. ChAT activity in hippocampus is significantly decreased following fimbria-fornix lesion compared to naïve mice and surgical controls. \* $p < 0.01$**

Fimbria-fornix lesioned mice had statistically significant decreases in hippocampal ChAT activity levels ( $p < 0.01$ ) compared to both naïve (49.3% decrease) and surgical control (38.5% decrease) experimental groups (Figure 5). ChAT activity levels in hippocampus were not significantly different between naïve and surgical control groups.

### 3.1.5 Fimbria fornix lesion results in increased soluble A $\beta$ 42 levels in hippocampus

The A $\beta$ 42 ELISA analysis was based on data from nine fimbria fornix lesioned mice, five surgical controls, and nine naïve mice (Table 2 and Figure 6). In the hippocampi of naïve mice, the average amount of soluble A $\beta$ 42 was 11.51 $\pm$ 3.68 pg/mg. In the fimbria fornix lesioned mice,

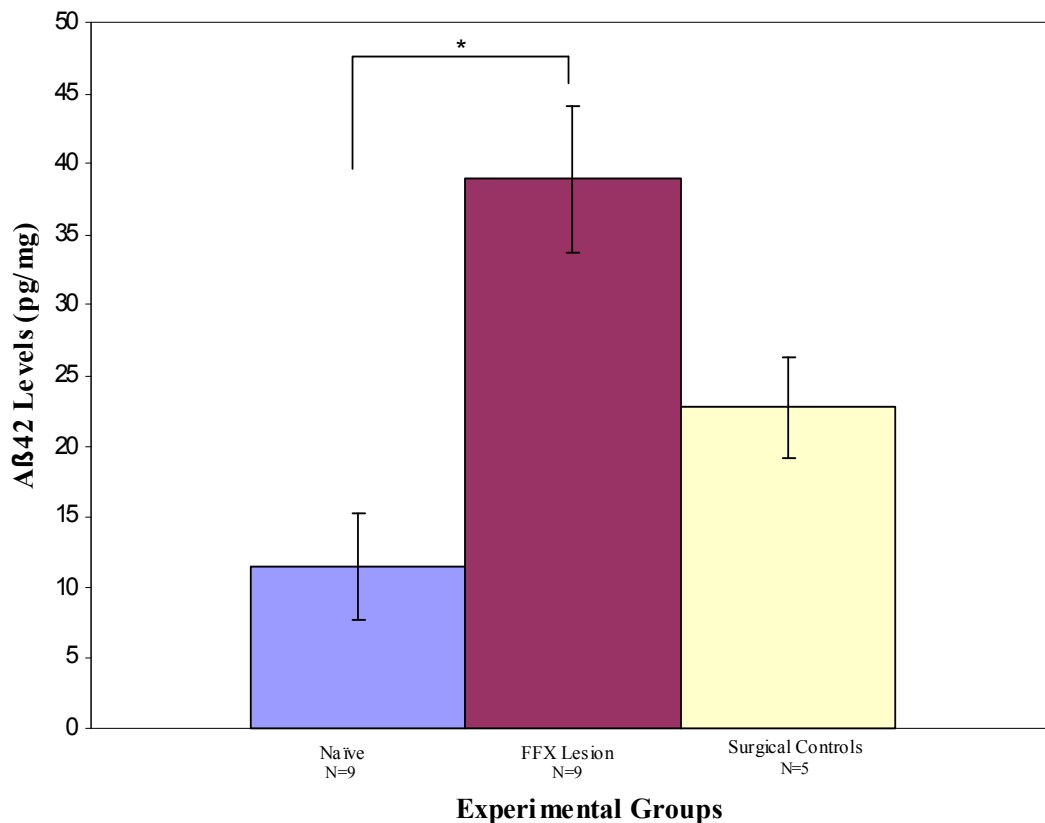


**Figure 6. Effect of bilateral fimbria-fornix on soluble A $\beta$ 42 levels in hippocampus. There was a significant increase in soluble A $\beta$ 42 levels in fimbria-fornix lesioned mice compared to naïve animals. \*p<0.01**

the average amount of soluble A $\beta$ 42 in hippocampus was 38.88 $\pm$ 5.20 pg/mg, a statistically significant (p<0.01) three-fold increase over naïve mice. In the surgical control group, the mean amount of soluble A $\beta$ 42 in hippocampus was 22.71 $\pm$ 3.63 pg/mg. Compared to surgical controls,

the fimbria fornix lesioned mice had almost double the amount of soluble A $\beta$ 42, although this increase was not statistically significant.

### 3.1.6 Correlative analyses

Correlative analyses were performed to determine possible relationships among ChAT activity, AChE activity and soluble A $\beta$ 42 levels. There was a statistically significant correlation between ChAT and AChE activity levels ( $r=0.85$ ,  $p<.0001$ ) in hippocampi of animals from all three experimental groups (Figure 7).

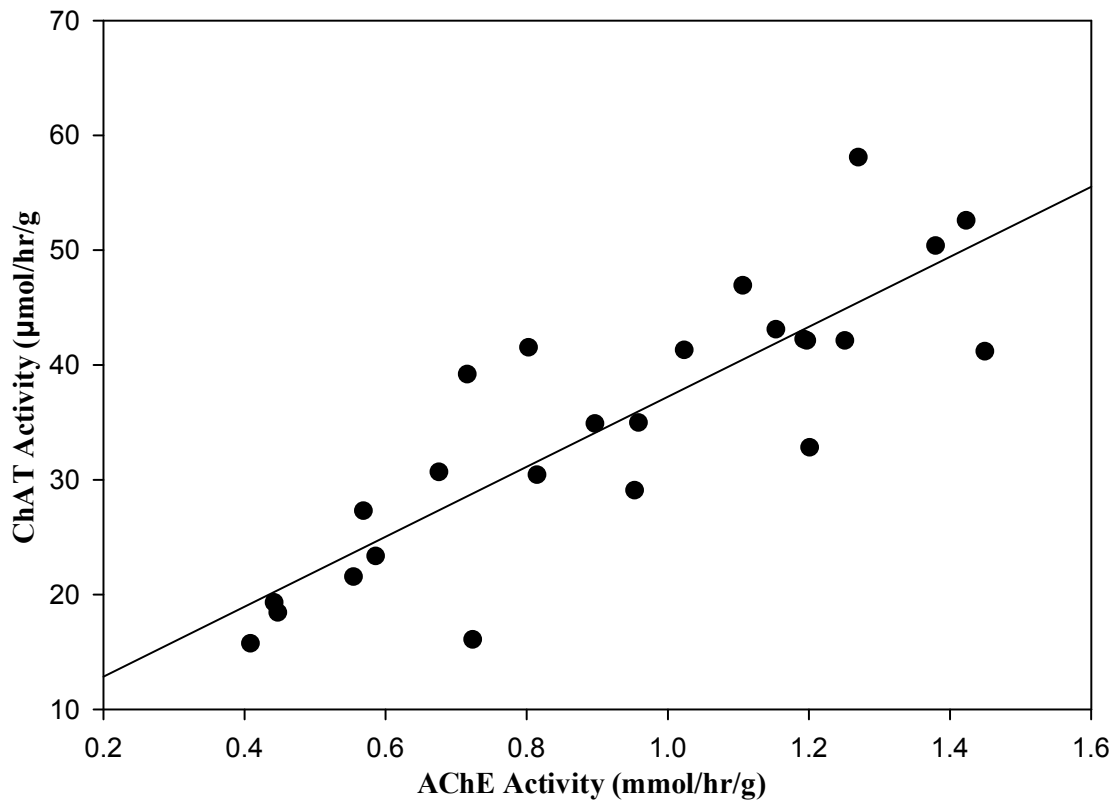


**Figure 7. ChAT activity increases as AChE activity increases. There is a significant direct correlation between these two cholinergic enzymes.  $r=0.85$ ,  $p<0.0001$**

There was a strong and significant correlation ( $r=-0.6974$ ,  $p<.0001$ ) between lower AChE activity and elevated soluble A $\beta$ 42 levels (Figure 8), and between lower ChAT activity and increased soluble A $\beta$ 42 levels ( $r=-0.7285$ ,  $p<.0001$ ; Figure 9). These correlative analyses, taken together, indicate that increases in hippocampal soluble A $\beta$ 42 levels are a result of reduced cholinergic projections and activity to the hippocampus.

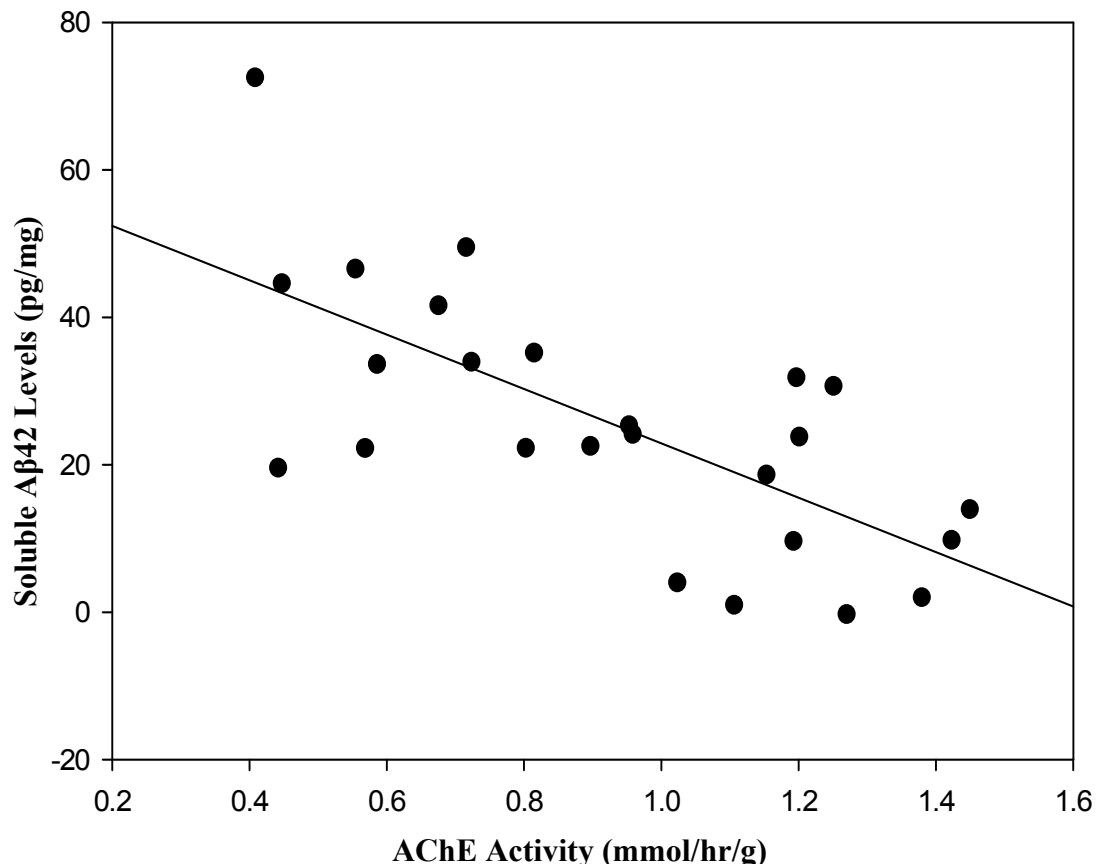


**Figure 8. Soluble A $\beta$ 42 levels increase as AChE activity decreases. There is a significant negative correlation between lower AChE activity and increased soluble A $\beta$ 42 levels in the hippocampus in animals from three experimental groups.  $r=-0.6974$ ,  $p<0.0001$**

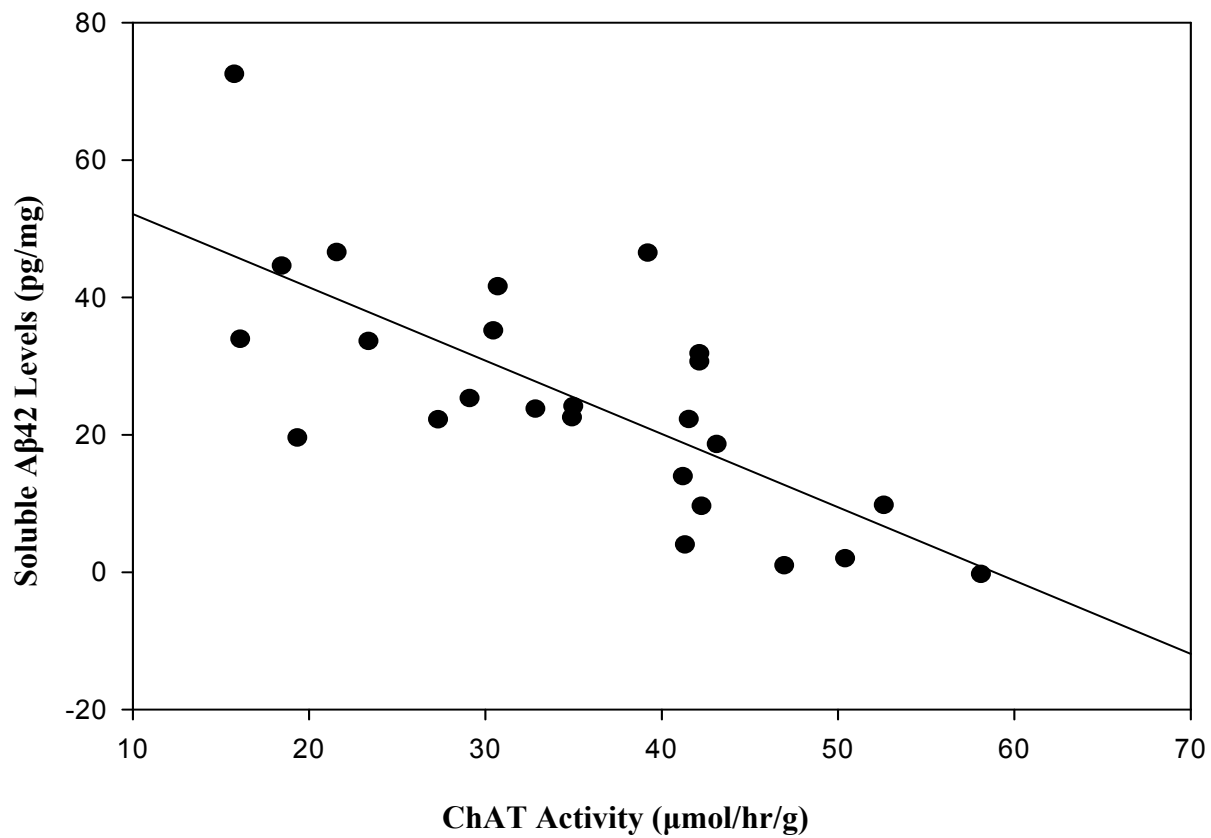


**Figure 9. Soluble Aβ42 levels increase as ChAT activity decreases.**  
**There is a significant negative correlation between increased soluble Aβ42 levels and decreased ChAT enzyme activity in the hippocampus from three experimental groups.  $p < 0.0001$**

## 4.0 DISCUSSION

In this study, we investigated whether decreasing cholinergic activity affects soluble A $\beta$  levels in hippocampus. Previous studies have suggested that activating cholinergic neurotransmission results in a shift of APP processing towards the non-amyloidogenic pathway, causing an increase in levels of sAPP $\alpha$  and a decrease in levels of A $\beta$  (Caccamo A et al, 2006). This is thought to be neuroprotective, because sAPP $\alpha$  is considered beneficial, and A $\beta$  harmful to neurons (Lahiri DK et al, 2007). Earlier studies demonstrated that removing cholinergic input into hippocampus, either by fimbria fornix lesion or injection of excitotoxins to the cholinergic basal forebrain, increased hippocampal APP mRNA and protein levels (Beeson JG et al, 1994; Lin L et al, 1999).

The present study tested the hypothesis that depriving the hippocampus of its cholinergic input, via bilateral fimbria fornix lesion, would result in increased levels of A $\beta$ 42 peptide in that brain region. We conducted our analyses at 2.5 weeks following surgery, because a number of studies in rodents have reported that at this time point there are significant decreases in AChE and ChAT enzyme activity levels in the hippocampus (Häge B et al, 1996; Liu L et al, 2002). We demonstrated a significant decrease of ChAT-immunoreactive fibers in hippocampus from fimbria fornix lesioned animals compared to naïve mice. The validity of our model, regarding the extent of reduction in cholinergic input to hippocampus at this time post-lesion, was further confirmed by biochemical assays of AChE and ChAT enzyme activities in the hippocampus. There was not a complete loss of cholinergic enzyme activity and this is consistent with evidence

in the literature. Partial fimbria-fornix lesions result in a sparing of some cholinergic fibers and lead to a significant, although not complete, decline in cholinergic enzyme activity (Piovesan P et al, 1995). There was not a significant change in ChAT or AChE activity levels in the surgical controls compared to the unoperated group, indicating that bilateral corpus callosum lesions did not interfere with cholinergic innervation in hippocampus. Thus, using a variety of histological, immunohistochemical, and biochemical methods we were able to demonstrate that our fimbria fornix lesioned animals have significantly reduced levels of cholinergic markers.

Once it was determined in our mouse model that the fimbria fornix lesion reduced cholinergic input into hippocampus, A $\beta$  levels in that region were measured. Specifically, we focused on measuring changes in soluble A $\beta$ 42 peptide. Soluble A $\beta$  has recently been shown to adversely affect long-term potentiation and synapses (Klyubin I et al, 2005; Lindner MD et al, 2006; Lahiri DK et al, 2007). Increasingly, cognitive problems seen in AD are thought to be related primarily to increased levels of soluble A $\beta$  and its oligomers (McLean CA et al, 1999). Because A $\beta$ 42 is abundantly produced in AD, and the cholinergic system is affected very early in the disease course, decreased cholinergic neurotransmission may be related to increased levels of soluble A $\beta$ 42. Using an ELISA, we found a significant increase in soluble A $\beta$ 42 levels in hippocampus of fimbria fornix lesioned animals. There was also a nonsignificant increase in soluble A $\beta$ 42 in fimbria fornix lesioned animals compared to surgical controls. The slight increase in A $\beta$ 42 in the surgical controls was not unexpected. Axons in the cingulate bundle innervate the hippocampus at the temporal pole (Gulyas AI et al, 1999). When lesioning corpus callosum, some adjacent white matter tracts, including cingulate bundle and hippocampal commissure, may be partially affected. This, together with the known response of increased APP

accumulation following injury (Ciallella JR et al, 2002) might result in elevated A $\beta$  levels in hippocampus.

The most persuasive results of this study were revealed by the correlative analyses of changes in ChAT and AChE enzyme activities and soluble A $\beta$ 42 levels. The strong direct correlation between ChAT and AChE activity levels indicated that both enzymes were equally affected by the lesion, consistent with the loss of cholinergic fiber input to the hippocampus. Cholinergic enzyme activity decline correlated strongly with increased soluble A $\beta$ 42 levels, supporting the hypothesis that impaired cholinergic function enhances amyloidogenic processing of APP in the hippocampus. These observations have considerable clinical and pathological implications suggesting that impaired cholinergic neurotransmission precedes, and may augment development of amyloid pathology in denervated brain regions.

Previous studies employed the fimbria fornix lesion model of cholinergic denervation in transgenic mice, which over-express mutant forms of human APP and deposit A $\beta$  plaques, but failed to show changes in numbers of A $\beta$  plaques (Liu L et al, 2002). The mutant APP overexpressors used in these studies do not allow for detecting subtle changes in A $\beta$  levels; in response to the lesion, these animals may produce A $\beta$  levels that are difficult to discern from the constant APP over-production associated with this transgene. In contrast, our humanized A $\beta$  mice produce human A $\beta$  without concomitant overexpression of APP, which allows detection of even slight changes in A $\beta$  production (Reaume AG et al, 1996).

Cholinergic enhancing drugs have been the most promising interventions in symptomatic AD. Early cholinergic therapies (Tacrine) had beneficial effects on cognition although these drugs had significant side effects and hepatic toxicity. The second generation of cholinergic therapies more specifically targeted the central cholinergic system, with fewer peripheral side

effects. Recently, Caccamo et al reported beneficial results of using a selective M1 agonist in a triple transgenic mouse. This drug (AF267B) was effective not only in reducing A $\beta$  plaques and tangles, but also in overcoming cognitive deficits in those mice (Caccamo A et al, 2006). Therefore, the interplay between enhanced cholinergic neurotransmission and A $\beta$  production warrants further investigation to develop effective therapies for AD.

Our results indicate that A $\beta$  levels in vivo are influenced by cholinergic system modulation, and that deficient cholinergic innervation of the hippocampus results in increased levels of soluble A $\beta$ 42, although the exact mechanism responsible is not clear and needs to be investigated. Studies indicate that the increase in A $\beta$  is a result of decreased production of sAPP $\alpha$ , a consequence of reduced cholinergic neurotransmission. Hippocampi from hA $\beta$  mice which have undergone fimbria-fornix lesions need to be analyzed for levels of sAPP $\alpha$ , sAPP $\beta$  as well as total APP. In addition, changes in  $\alpha$ -secretase activity following fimbria-fornix lesions need to be measured. Subsequent experiments should examine changes in  $\alpha$ -secretase activity following combination of lesions and pharmacological intervention (i.e. cholinergic agonist). The results of these studies will indicate how cholinergic denervation affects APP metabolism.

Another important follow-up set of experiments would involve hA $\beta$  mice which also contain the PS1 mutation and form A $\beta$  plaques, to examine whether 1) lesioning fimbria fornix can enhance A $\beta$  plaque deposition under these conditions, and 2) muscarinic agonist intervention can reduce soluble A $\beta$  levels and decrease A $\beta$  plaque deposits in the neuropil. In addition to reducing A $\beta$  levels, behavioral tests would be performed to see if the cholinergic agonist can overcome the cognitive impairments which occur following fimbria fornix lesions (Galani R et al, 2002). The results of these studies would help to better understand the relationship between

cholinomimetic drug therapy and how it affects progression of neurotoxic A $\beta$  pathology in AD patients.

## REFERENCES

Alonso JR, U HS and Amaral DG. (1996) Cholinergic innervation of the primate hippocampal formation: II. Effects of fimbria/fornix transection. *J Comp Neurol* 375(4):527-51

Apelt J, Kumar A, and Schliebs R. (2002) Impairment of cholinergic neurotransmission in adult and aged transgenic Tg2576 mouse brain expressing the Swedish mutation of human  $\beta$ -amyloid precursor protein. *Brain Res* 953:17-30.

Aucoin JS, Jiang P, Aznavour N, Tong XK, Buttini M, Descarries L and Hamel E. (2005) Selective cholinergic denervation, independent from oxidative stress, in a mouse model of Alzheimer's disease. *132*:73-86.

Auld DS, Kar S, and Quirion R. (1998)  $\beta$ -amyloid peptides as direct cholinergic neuromodulators: a missing link? *TINS* 21(1):43-49.

Auld DS, Kornecook TJ, Bastianetto S, and Quirion R. (2002) Alzheimer's disease and the basal forebrain cholinergic system: relations to  $\beta$ -amyloid peptides, cognition, and treatment strategies. *Prog Neurobio* 68: 209-245.

Ballard CG, Chalmers KA, Todd C, McKeith IG, O'Brien JT, Wilcock G, Love S and Perry EK. (2007) Cholinesterase inhibitors reduce cortical A $\beta$  in dementia with Lewy bodies. *Neurology* 68:1726-1729.

Buxbaum JD, Oishi M, Chen HI, Pinkas-Kramarski R, Jaffe EA, Gandy SE and Greengard P. (1992) Cholinergic agonists and interleukin 1 regulate processing and secretion of the Alzheimer  $\beta$ /A4 amyloid protein precursor. *PNAS* 89:10075-10078.

Beeson JG, Shelton ER, Chan HW and Gage FH. (1994) Age and damage induced changes in amyloid protein precursor immunohistochemistry in the rat brain. *J Comp Neurol* 342:69-77.

Bigl M, Apelt J, Lushekina EA, Lange-Dohna C, Roßner S and Schliebs R. (2000) Expression of  $\beta$ -secretase mRNA in transgenic Tg2576 mouse brain with Alzheimer plaque pathology. *Neuroscience Letters* 292(2):107-110.

Blaker SN, Armstrong DM and Gage FH. (1988) Cholinergic neurons within the rat hippocampus: response to fimbria-fornix transaction. *J Comp Neurol* 272:127-138.

Caccamo A, Oddo S, Billings LM, Green KN, Martinez-Corla H, Fisher A and LaFerla F. (2006) M1 Receptors Play a Central Role in Modulating AD-like Pathology in Transgenic Mice. *Neuron* 49:671-682.

Chang EH, Savage MJ, Flood DG, Thomas JM, Levy RB, Mahadomrongkul V, Shirao T, Aoki C and Huerta PT. (2006) AMPA receptor downscaling at the onset of Alzheimer's disease pathology in double knockin mice. *PNAS* 103(9):3410-3415.

Chen XH, Siman R, Iwata A, Meaney DF, Trojanowski JQ, Smith DH. (2004) Long-term accumulation of amyloid-beta, beta-secretase, presenilin-1, and caspase-3 in damaged axons following brain trauma. *Am J Pathol.* 165(2):357-71.

Cummings JL (2000) The role of cholinergic agents in the management of behavioural disturbances in Alzheimer's disease. *Int J Neuropsychopharmacol* 3(7):21-29.

De Lacalle S, Lim C, Sobreviela T, Mufson EJ, Hersh LB, Saper CB. (1994) Cholinergic innervation in the human hippocampal formation including the entorhinal cortex. *J Comp Neurol.* 345(3):321-44.

DeKosky ST, Scheff SW, Markesbery WR. (1985) Laminar organization of cholinergic circuits in human frontal cortex in Alzheimer's disease and aging. *Neurology.* 35(10):1425-31.

DeKosky ST and Scheff SW. (1990) Synapse loss in frontal cortex biopsies in Alzheimer's disease: correlation with cognitive severity. *Ann Neurol* 27:457-464.

DeKosky ST, Ikonomic MD, Styren SD, Beckett L, Wisniewski S, Bennett DA, Cochran EJ, Kordower JH and Mufson EJ. (2002) Upregulation of choline acetyltransferase

activity in hippocampus and frontal cortex of elderly subjects with mild cognitive impairment. *Ann Neurol* 51(2):145-55.

DeKosky ST, Kaufer DI and Lopez OL. (2004) The dementias. *Neurology in Clinical Practice*, 4th Edition . W.G. Bradley, R.B. Daroff, G.M. Fenichel, and J. Jankovic, Editors. Philadelphia: Butterworth Heinemann, 1901-1951.

Ellman GL, Courtney D, Andres Jr V and Featherstone RM. (1961) A new and rapid colorimetric determination of acetylcholinesterase activity. *Biochem Pharmacol* 7:88-95.

Fonnum F. (1975) A rapid radiochemical method for the determination of choline acetyltransferase. *J Neurochem.* 24(2):407-9.

Fuxe K, Rosén L, Lippoldt A, Andbjør B, Hasselrot U, Finnman UB and Agnati LF. (1994) Chronic continuous infusion of nicotine increases the disappearance of choline acetyltransferase immunoreactivity in the cholinergic cell bodies of the medial septal nucleus following a partial unilateral transection of the fimbria fornix. *Clin Investig.* 72(4):262-8

Galani R, Obis S, Coutureau E, Jarrard L, Cassel JC. (2002) A comparison of the effects of fimbria-fornix, hippocampal, or entorhinal cortex lesions on spatial reference and working memory in rats: short versus long postsurgical recovery period. *Neurobiol Learn Mem.* 77(1):1-16.

German DC, Yazdani U, Speciale SG, Pasbakhsh P, Games D, Liang CL. (2003) Cholinergic neuropathology in a mouse model of Alzheimer's disease. *J Comp Neurol.* 462(4):371-81.

Ginsberg SD and Martin LJ. (1998) Ultrastructural analysis of the progression of neurodegeneration in the septum following fimbria-fornix transection. *Neuroscience* 86(4):1259-72.

González I, Arévalo-Serrano J, Sanz-Anquela JM and Gonzalo-Ruiz A. (2007) Effects of  $\beta$ -amyloid protein on M1 and M2 subtypes of muscarinic acetylcholine receptors in the medial septum-diagonal band complex of the rat: relationship with cholinergic, GABAergic, and calcium-binding protein perikarya. *Acta Neuropath* 113:637-651.

Gouras GK, Almeida CG and Takahashi RH. (2005) Intraneuronal A $\beta$  accumulation and origin of plaques in Alzheimer's disease. *Neurobio Aging* 26:1235-1244.

Greig NH, Utsuki T, Ingram DK, Wang Y, Pepeu G, Scali C, Yu QS, Mamczarz J, Holloway HW, Giordano T, Chen D, Furukawa K, Sambamurti K, Brossi A and Lahiri DK. (2005) Selective butyrylcholinesterase inhibition elevates brain acetylcholine, augments learning and lowers Alzheimer beta-amyloid peptide in rodent. *PNAS* 102(47):17213-17218.

Gulyás AI, Acsády L, Freund TF. (1999) Structural basis of the cholinergic and serotonergic modulation of GABAergic neurons in the hippocampus. *Neurochem Int.* 34(5):359-72.

Haass C and Selkoe DJ. (1993) Cellular processing of  $\beta$ -amyloid precursor protein and the genesis of amyloid  $\beta$ -peptide. *Cell* 75:1039-1042.

Häge B, Frotscher M and Naumann T. (1996) Activity of choline acetyltransferase in the rat medial septal nucleus following fimbria-fornix transection or selective immunolesioning with 192 IgG saporin. *Neurosci Letters* 205:119-122.

Harigaya Y, Tomidokoro Y, Ikeda M, Sasaki A, Kawarabayashi T, Matsubara E, Kanai M, Saido TC, Younkin SG, Shoji M. (2006) Type-specific evolution of amyloid plaque and angiopathy in APPsw mice. *Neurosci Lett.* 395(1):37-41.

Haroutunian V, Greig N, Pei XF, Utsuki T, Gluck R, Acevedo LD, Davis KL, and Wallace WC. (1997) Pharmacological modulation of Alzheimer's  $\beta$ -amyloid precursor protein levels in the CSF of rats with forebrain cholinergic system lesions. *Molec Brain Res* 46:161-168.

Hellström-Lindahl E. (2000) Modulation of  $\beta$ -amyloid precursor protein processing and tau phosphorylation by acetylcholine receptors. *Euro J Pharmacology* 393:255-263.

Holtzman DM, Li Y, DeArmond SJ, McKinley MP, Gage FH, Epstein CJ and Mobley WC. (1992) Mouse model of neurodegeneration: Atrophy of basal forebrain cholinergic neurons in trisomy 16 transplants. PNAS 89:1383-1387.

Holscher C, Gengler S, Gault VA, Harriott P and Mallot HA. (2007) Soluble beta-amyloid[25-35] reversibly impairs hippocampal synaptic plasticity and spatial learning. Euro J Pharmacol 561:85-90.

Hoover DB, Muth EA and Jacobowitz DM. (1978) A mapping of the distribution of acetylcholine, choline acetyltransferase and acetylcholinesterase in discrete areas of rat brain. Brain Res. 153(2):295-306.

Ikonomovic MD, Abrahamson EE, Isanski BA, Wu J, Mufson EJ and DeKosky ST. (2007) Superior frontal cortex cholinergic axon density in mild cognitive impairment and early Alzheimer disease. Arch Neurol 64(9):1312-7.

Jin K, Galvan V, Xie L, Mao XO, Gorostiza OF, Bredesen DE and Greenberg DA. (2004) Enhanced neurogenesis in Alzheimer's disease transgenic (PDGF-APP<sup>Sw,Ind</sup>) mice. PNAS 101(36):13363-7.

Kamenetz F, Tomita T, Hsieh H, Seabrook G, Borchelt, Iwatsubo T, Sisodia S, and Malinow. (2003) APP Processing and Synaptic Function. Neuron 37: 925-937.

Kar S, Issa MA, Seto D, Auld DS, Collier B and Quirion R. (1998) Amyloid  $\beta$ -peptide inhibits high-affinity choline uptake and acetylcholine release in rat hippocampal slices. *J Neurochem* 70:2179-2187.

Kimberly WT, LaVoie MJ, Ostaszewski BL, Ye W, Wolfe MS and Selkoe DJ. (2003) Gamma-secretase is a membrane protein complex comprised of presenilin, nicastrin, Aph-1, and Pen-2. *Proc Natl Acad Sci U S A.* 100(11):6382-7.

Klinger M, Apelt J, Kumar A, Sorger D, Sabri O, Steinbach J, Scheunnemann M and Schliebs R. (2003) Alterations in cholinergic and non-cholinergic neurotransmitter receptor densities in transgenic Tg2576 mouse brain with  $\beta$ -amyloid plaque pathology. *Int J Devl Neuroscience* 21:357-369.

Klyubin I, Walsh DM, Lemere CA, Cullen WK, Shankar GM, Betts V, Spooner ET, Jiang L, Anwyl R, Selkoe DJ and Rowan MJ. (2005) Amyloid beta protein immunotherapy neutralizes Abeta oligomers that disrupt synaptic plasticity in vivo. *Nat Med* 11(5):556-61.

Lacor PN, Buniel MC, Chang L, Fernandez SJ, Gong Y, Viola KL, Lambert MP, Velasco PT, Bigio EH, Finch CE, Krafft GA and Klein WL. (2004) Synaptic targeting by Alzheimer's-related amyloid  $\beta$  oligomers. *J Neurosci* 24(45):10191-10200.

Lahiri DK, Chen DM, Maloney B, Holloway HW, Yu Q, Utsuki T, Giordano T, Sambamurti K and Greig NH. (2007) The experimental Alzheimer's Disease drug posiphen [(+)-Phenserine] lowers amyloid- $\beta$  peptide levels in cell culture and mice. *J Pharm Experimental Techniques* 320(1):386-396.

Lapchak PA, Jenden DJ, and Hefti F. (1991) Compensatory elevation of acetylcholine synthesis *in vivo* by cholinergic neurons surviving partial lesions of the septohippocampal pathway. *J Neurosci* 11(9):2821-2828.

Lazarov O, Lee M, Peterson DA, and Sisodia SS. (2002) Evidence that synaptically released  $\beta$ -amyloid accumulates as extracellular deposits in the hippocampus of transgenic mice. *J Neuroscience* 22(22):9785-9793.

Lesné S, Koh MT, Kotilinek L, Kaye R, Glabe CG, Yang A, Gallagher M and Ashe KH. (2006) A specific amyloid- $\beta$  protein assembly in the brain impairs memory. *Nature* 440:352-357.

Lewis PR, Shute CC, and Silver A. Confirmation from choline acetyltransferase analyses of a massive cholinergic innervation to the rat hippocampus. *J Physiol* 191: 215-224.

Lin L, LeBlanc CJ, Deacon TW and Isaacson O. (1998) Chronic cognitive deficits and amyloid precursor protein elevation after selective immunotoxin lesions of the basal forebrain cholinergic system. *NeuroReport* 9:547-552.

Lin L, Georgievska B, Mattsson A and Isaacson O. (1999) Cognitive changes and modified processing of amyloid precursor protein in the cortical and hippocampal system after cholinergic synapse loss and muscarinic receptor activation. *PNAS* 96(21):12108-12113.

Lindner MD, Hogan JB, Krause RG, Machet F, Bourin C, Hodges, Jr DB, Corsa JA, Barten DM, Toyn JH, Stock DA, Rose GM and Gribkoff VK. (2006) Soluble A $\beta$  and cognitive function in aged F-344 rats and Tg2576 mice. *Behav Brain Res* 173:62-75.

Ling Y, Morgan K, and Kalsheker N. (2003) Amyloid precursor protein and the biology of proteolytic processing: relevance to Alzheimer's Disease. *Int J Biochem Cell Biol* 35: 1505-1535.

Liskowsky W and Schliebs R. (2006) Muscarinic acetylcholine receptor inhibition in transgenic Alzheimer-like Tg2576 mice by scopolamine favours the amyloidogenic route of processing of amyloid precursor protein. *Int J Devl Neurosci* 24:149-156.

Liu L, Ikonen S, Tapiola T, Tanila H and van Groen T. (2002) Fimbria-fornix lesion does not affect APP levels and amyloid deposition in the hippocampus of APP+PS1 double transgenic mice. *Exp Neurol*. 177(2):565-74.

Lüth HJ, Apelt J, Ihunwo AO, Arendt T, and Schliebs R. (2003) Degeneration of  $\beta$ -amyloid-associated cholinergic structures in transgenic APP<sub>SW</sub> mice. *Brain Res* 977:16-22.

Mesulam MM, Mufson EJ, Levey AI, Wainer BH. (1983) Cholinergic innervation of cortex by the basal forebrain: cytochemistry and cortical connections of the septal area, diagonal band nuclei, nucleus basalis (substantia innominata), and hypothalamus in the rhesus monkey. *J Comp Neurol* 214(2):170-97.

Mesulam M. (2004) The Cholinergic lesion of Alzheimer's Disease: pivotal factor or side show? *Learn Mem* 11(1):43-9.

McKinney M, Coyle JT and Hedreen JC. (1983) Topographic analysis of the innervation of the rat neocortex and hippocampus by the basal forebrain cholinergic system. *J Comparative Neurol* 217:103-121.

McLean CA, Cherny RA, Fraser FW, Fuller SJ, Smith MJ, Beyreuther K, Bush AI and Masters CL. (1999) Soluble pool of A $\beta$  Amyloid as a determinant of severity of neurodegeneration in Alzheimer's disease. *Ann Neurol* 46:860-866.

Mountjoy CQ. (1986) Correlations between neuropathological and neurochemical changes. *Br Med Bull.* 42(1):81-5.

Naslund J, Haroutunian V, Mohs R, Davis KL, Davies P, Greengard P and Buxbaum JD. (2000) Correlation between elevated levels of amyloid beta-peptide in the brain and cognitive decline. *JAMA* 283(12):1571-7.

Oda Y. (1999) Choline acetyltransferase: the structure, distribution and pathologic changes in the central nervous system. *Pathol Int.* 49(11):921-37

Oddo S, Caccamo A, Tran L, Lambert MP, Glabe CG, Klein WL and LaFerla FM. (2006) Temporal profile of amyloid- $\beta$  (A $\beta$ ) oligomerization in an *in vivo* model of Alzheimer's disease. *J Bio Chem* 281(3):1599-1604.

Pakaski M and Kasa P. (2003) Role of Acetylcholinesterase Inhibitors in the Metabolism of Amyloid Precursor Protein. *Curr Drug Targets CNS Neurol Dis* 2:163-171.

Piovesan P, Quatrini G, Pacifici L, Tagliatalata G and Angelucci L. (1995) Acetyl-L-carnitine restores choline acetyltransferase activity in the hippocampus of rats with partial unilateral fimbria-fornix transection. *Int J Dev Neurosci* 13(1):13-9.

Racchi M, Mazzucchelli M, Porrello E, Lanni C and Govoni S. (2004) Acetylcholinesterase inhibitors: novel activities of old molecules. *Pharmacol Res* 50:441-451.

Ramirez MJ, Ridley RM, Baker HF, Maclean CJ, Honer WG and Francis PT. (2001) Chronic elevation of amyloid precursor protein in the neocortex or hippocampus of marmosets with selective cholinergic lesions. *J Neural Trans* 108(7):809-826.

Reaume AG, Howland DS, Trusko SP, Savage MJ, Lang DM, Greenberg BD, Siman R and Scott RW. (1996) Enhanced amyloidogenic processing of the  $\beta$ -amyloid precursor protein in

gene targeted mice bearing the Swedish familial Alzheimer's disease mutations and a "humanized" A $\beta$  sequence. *J Bio Chem* 271(38):23380-23388.

Ren K, King MA, Liu J, Siemann J, Altman M, Meyers C, Hughes JA, Meyer EM. (2007) The alpha7 nicotinic receptor agonist 4OH-GTS-21 protects axotomized septohippocampal cholinergic neurons in wild type but not amyloid-overexpressing transgenic mice. *Neuroscience* 148(1):230-7.

Scheff SW, DeKosky ST and Price DA. (1990) Quantitative assessment of cortical synaptic density in Alzheimer's Disease. *Neurobio Aging* 11:29-37.

Schliebs R and Arendt T. (2006) The significance of the cholinergic system in the brain during aging and in Alzheimer's disease. *J Neural Trans* 113: 1625-1644.

Selkoe DJ. (2005) Defining molecular targets to prevent Alzheimer disease. *Arch Neurol* 62(2):192-5.

Shoji M, Golde TE, Ghiso J, Cheung TT, Estus S, Shaffer LM, Cai XD, McKay DM, Tintner R, Frangione B, and Younkin SG. (1992) *Science* 258:126-129.

Standridge JB. (2006) Vicious cycles within the neuropathophysiologic mechanisms of Alzheimer's disease. *Curr Alzheimer Res* 3(2):95-108.

Terry RD, Masliah E, Salmon DP, Butters N, DeTeresa R, Hill R, Hansen LA and Katzman R. (1991) Physical basis of cognitive alterations in Alzheimer's disease: synapse loss is the major correlate of cognitive impairment. *Ann Neurol* 30(4):572-80.

Tseng BP, Kitazawa M and LaFerla FM. (2004) Amyloid  $\beta$ -peptide: The inside story. *Curr Alz Res* 1:231-239.

Tweedie D, Brossi A, Chen D, Ge YW, Bailey J, Yu Q, Kamal MA, Sambamurti K, Lahiri D and Greig NH. (2006) Neurine, an acetylcholine autolysis product, elevates secreted amyloid-

van Groen T, Liu L, Ikonen S and Kadish I. (2003) Diffuse amyloid deposition, but not plaque number, is reduced in amyloid precursor protein/presenilin 1 double-transgenic mice by pathway lesions. *Neuroscience* 119(4):1185-97.

Vassar R, Bennett BD, Babu-Khan S, Kahn S, Mendiaz EA, Denis P, Teplow DB, Ross S, Amarante P, Loeloff R, Luo Y, Fisher S, Fuller J, Edenson S, Lile J, Jarosinski MA, Biere AL, Curran E, Burgess T, Louis JC, Collins F, Treanor J, Rogers G and Citron M. (1999) Beta-secretase cleavage of Alzheimer's amyloid precursor protein by the transmembrane aspartic protease BACE. *Science* 286(5440):735-41.

Wallace WC, Lieberburg I, Schenk D, Vigo-Pelfrey C, Davis KL, and Haroutunian V. (1995) Chronic elevation of secreted amyloid precursor protein in subcortically lesioned rats, and its exacerbation in aged rats. *J Neurosci* 15(7):4896-4905.

Walsh DM, Klyubin I, Fadeeva JV, Rowan MJ and Selkoe DJ (2002) Amyloid-beta oligomers: their production, toxicity and therapeutic inhibition. *Biochem Soc Trans.* 2002 30(4):552-7.

Whitehouse PJ, Price DL, Struble RG, Clark AW, Coyle JT and Delon MR. (1982) Alzheimer's disease and senile dementia: loss of neurons in the basal forebrain. *Science* 215(4537):1237-9.

Wong TP, Debeir T, Duff K and Cuello AC. (1999) Reorganization of cholinergic terminals in the cerebral cortex and the hippocampus in transgenic mice carrying mutated presenilin-1 and amyloid precursor protein. *J Neurosci* 19(7):2706-2716.

Zaborszky L, Zimmermann M, Borroni B, Cattabeni F, Padovani A, and Di Luca M. (2005) Cholinesterase inhibitors influence APP metabolism in Alzheimer disease patients. *Neurobiol Dis* 19:237-242.

Zimmermann M, Gardoni F and Di Luca M (2005) Molecular rationale for the pharmacological treatment of Alzheimer's disease. *Drugs Aging*. 22 Suppl 1:27-37.